J. Fluid Mech. (1995), *vol.* 282, *pp.* 339–371

Nonlinear evolution of a pair of oblique instability waves in a supersonic boundary layer

By S. J. LEIB AND SANG SOO LEE

NYMA Inc., Lewis Research Center Group, Cleveland, OH 44135, USA

(Received 15 April 1994 and in revised form 26 July 1994)

We study the nonlinear evolution of a pair of oblique instability waves in a supersonic boundary layer over a flat plate in the nonlinear non-equilibrium viscous critical layer regime. The instability wave amplitude is governed by the same integro-differential equation as that derived by Goldstein & Choi (1989) in the inviscid limit and by Wu, Lee & Cowley (1993) with viscous effects included, but the coefficient appearing in this equation depends on the mean flow and linear neutral stability solution of the supersonic boundary layer. This coefficient is evaluated numerically for the Mach number range over which the (inviscid) first mode is the dominant instability. Numerical solutions to the amplitude equation using these values of the coefficient are obtained. It is found that, for insulated and cooled wall conditions and angles corresponding to the most rapidly growing waves, the amplitude ends in a singularity at a finite downstream position over the entire Mach number range regardless of the size of the viscous parameter. The explosive growth of the instability waves provides a mechanism by which the boundary layer can break down. A new feature of the compressible problem is the nonlinear generation of a spanwise-dependent mean distortion of the temperature along with that of the velocity found in the incompressible case.

1. Introduction

The transition from laminar to turbulent flow in boundary layers has long been of great interest and significant progress has been made over the years toward developing an understanding of this process in incompressible flows. The corresponding problem at supersonic speeds is less well understood but recent technological applications have generated a renewed interest in these flows. In incompressible and subsonic compressible flows two-dimensional disturbances are generally the most rapidly growing linear disturbances and they tend to dominate the linear stage of the process. Three-dimensional effects usually develop further downstream in the form of a harmonic or subharmonic resonance involving the fundamental two-dimensional disturbance and a pair of oblique (three-dimensional) waves. Rapid growth of the three-dimensional component leads fairly quickly to transition to a turbulent boundary layer. In contrast, for moderately supersonic flows, where the so-called first mode is dominant (Mack 1984, 1987), oblique (three-dimensional) waves are the most rapidly growing in the initial linear stage. It is quite likely then that the onset of nonlinearity in these flows involves the interaction of oblique instability waves.

Transition is often studied experimentally, and, increasingly, by numerical simulation, by introducing controlled small-amplitude disturbances into the boundary

layer and following the subsequent downstream evolution of the flow. For sufficiently small-amplitude excitation the initial instability wave growth has been established as being well described by linear stability theory. The slow viscous spreading of the mean flow causes the local instability wave growth rate to decrease while the wave continues to amplify downstream. Under these circumstances nonlinear effects will first appear in the thin critical layer surrounding the position where the mean velocity is equal to the neutral phase speed once the local growth rate becomes sufficiently small. The amplitude will still be relatively small at the onset of nonlinearity in this scenario which is consistent with the observations of experiments and numerical simulations. The unsteady flow outside the critical layer remains essentially linear but the instability wave growth is completely determined by the nonlinear flow in the critical layer. Nonlinear critical layer analyses have been carried out to describe the nonlinear evolution of initially linear instability waves in a variety of shear flows. For a review and further development of the works concerned specifically with the interaction of oblique waves see Goldstein (1994 *a*, *b*).

The first nonlinear critical layer analysis for a pair of oblique waves was carried out by Goldstein & Choi (1989, referred to herein as GC) for Rayleigh waves in an incompressible shear layer. They showed that nonlinear effects first appear when the growth rate becomes of the order $\epsilon^{1/3}$ where $\epsilon \ll 1$ is the characteristic instability wave amplitude in the nonlinear region. Their analysis showed that the instability wave amplitude is governed by a nonlinear integro-differential equation of the type first obtained by Hickernell (1984) for Rossby waves. Numerical solutions to the inviscid equation showed that the amplitude develops a singularity at a finite downstream distance and an asymptotic solution valid near the singularity was obtained. This explosive growth of the instability wave amplitude, if not suppressed by some additional effect, could result in a rapid breakdown of the laminar flow. They also showed that, as a consequence of the nonlinear interactions in the critical layer, a spanwise-dependent mean distortion of streamwise velocity is generated in the outer region at the same order as the primary disturbance. Wu, Lee & Cowley (1993) (hereafter referred to as WLC) extended the analysis of GC to include viscous effects within the critical layer in the context of an unsteady Stokes layer. They found that, for certain combinations of parameters, viscous effects eliminate the singularity and cause an exponential decay of the amplitude.

Unlike the subsonic case there are relatively few experimental studies of the transition process in supersonic boundary layers. Those that have been conducted were concerned mainly with the initial linear instability and with comparing their observations with the results of linear theory. Among the first experiments to examine the linear stability of supersonic flat plate boundary layers were those of Demetriades (1960) and Laufer & Vrebalovich (1960) who detected growing wave-like disturbances within the boundary layer and determined the upper and lower instability boundaries. Laufer & Vrebalovich (1960) further made quantitative comparisons with the early theoretical work of Lees & Lin (1946), Lees (1947) and Dunn & Lin (1955) and found reasonably good agreement at the relatively low supersonic Mach numbers considered. More recent experiments by Lysenko & Maslov (1984) and Kosinov, Maslov & Shevelkov (1990) have verified other features predicted by linear theory, for example the effect of wall cooling and the importance of oblique waves. Data from these later experiments have mostly been compared with the numerical solutions of the linear compressible stability equations obtained by Mack (1984, 1987).

Much of the information available concerning subsequent nonlinear stages in the supersonic transition process has come from numerical simulations. The simulations of Bestek, Thumm & Fasel (1992) and Ng & Zang (1993) suggest that the subharmonic resonance or secondary instability mechanisms that operate in subsonic flows are significantly weaker in the supersonic case where a much larger-amplitude primary disturbance is needed to effect the growth of secondary disturbances. Considering the dominance of oblique first mode waves, and in view of the possibility of explosive growth predicted by the nonlinear analyses of GC and WLC, it might be expected that the interaction of a pair of oblique instability waves provides a stronger mechanism by which moderately supersonic boundary layers can break down. A numerical simulation of the spatial evolution of a supersonic boundary layer subject to an initially small-amplitude pair of oblique waves with equal streamwise wavenumber and frequency and equal but opposite spanwise wavenumbers has recently been carried out by Bestek *et al.* (1992) using the full compressible Navier–Stokes equations. Chang & Malik (1992) carried out calculations for this problem using a parabolized approximation to the governing equations.

In this paper we consider the nonlinear critical layer interaction of a pair of oblique instability waves in a supersonic boundary layer. We will consider only the inviscid first mode instability so that, based on the linear stability results presented by Mack (1984, 1987), our results can be expected to apply for Mach numbers greater than about 2.5. It was also shown by Mack (1984) that the supersonic boundary layer can support additional inviscid instability modes for Mach numbers beyond about 3. Among these the second mode has a larger linear growth rate than the first mode for Mach numbers greater than about 4. The second mode is most rapidly growing as a two-dimensional wave so that its nonlinear evolution would be described by an analysis of the type carried out by Goldstein & Leib (1989) and Leib (1991) for a single wave in a supersonic flow rather than the oblique mode interaction considered here. However, in supersonic wind tunnel experiments the second mode is often not observed until the Mach number exceeds about 6 (Kendall 1975). It was pointed out by Reshotko (1969) that the second mode appears at very high frequency in such experiments and it has been suggested that its absence may be due to a lack of energy in the background disturbance environment at these very high frequencies (see also Mack 1975). Moreover, as far as the initiation of nonlinear effects is concerned, it is the integrated linear growth over many streamwise wavelengths that is relevant and in this sense the first mode dominates the second for Mach numbers up to about 6 or 7 (Malik 1989; Balakumar & Malik 1992). In practice then, the first mode oblique wave interaction provides a possible mechanism by which a supersonic boundary layer can break down for Mach numbers up to at least 6.

Compressibility effects do not alter the nonlinear terms in the critical layer equations which contribute to the velocity jump so that the kernel function appearing in the amplitude equation is the same as that given by GC and WLC. Additional linear terms appear due to non-zero temperature variations and these affect the coefficients appearing in the amplitude equation which determine the ultimate form of the solution. The evaluation of these coefficients for the supersonic boundary layer case is one of the main purposes of this paper. It is found that, for angles corresponding to the most rapidly growing waves, the values of these coefficients are such that the singularity in the instability wave amplitude cannot be eliminated by viscous effects no matter how large. A new feature of the compressible problem is the generation of a spanwise-dependent mean temperature distortion at the order of the primary disturbance in addition to that in the streamwise velocity. We will present

some detailed results for the mean distortion component which have not been given elsewhere. The results of recent numerical simulations of supersonic boundary layer stability by Erlebacher & Hussaini (1990) and Bestek *et al.* (1992) are consistent with the predictions of the critical layer theory.

In §2 we formulate the problem and present the solution in the region outside the critical layer. The equations governing the spanwise-dependent mean component are also given. The flow in the critical layer is considered in §3. Matching the velocity jumps from the critical layer and outer solutions yields the amplitude evolution equation which is discussed in §4. Numerical results are presented in §5 and a discussion of these and the analysis as applied to a supersonic boundary layer is contained in §6.

2. Formulation and outer solution

Consider the flow of an ideal gas over a flat plate with uniform free stream temperature T_∞ and velocity U_∞. The streamwise, transverse and spanwise coordinates, made dimensionless with the boundary layer thickness δ, are denoted by x, y and z, respectively, the corresponding velocity components are u, v and w, referred to the free stream velocity, and the time, normalized with δ/U_∞, is t. We will denote the pressure, temperature, viscosity and density by p, T, μ and ρ, respectively, using their values in the free stream as reference quantities. We define the free stream Mach number as

$$M = U_\infty/c_\infty, \tag{2.1}$$

and the Reynolds number as

$$R = U_\infty \delta/\nu_\infty, \tag{2.2}$$

where

$$c_\infty = (\gamma \Re T_\infty)^{1/2}, \tag{2.3}$$

and ν_∞ are the speed of sound and kinematic viscosity in the free stream respectively, γ is the isentropic exponent of the gas and $\Re$ is the gas constant. The local Prandtl number (assumed to be constant) is defined as

$$\sigma_0 = \mu c_p/\kappa, \tag{2.4}$$

where c_p and κ are the normalized specific heat, and thermal conductivity, respectively.

The governing momentum, continuity and energy equations, in terms of these normalized variables, are

$$\frac{\mathrm{D}U_i}{\mathrm{D}t} = -\frac{1}{\rho\gamma M^2}\frac{\partial p}{\partial X_i} + \frac{1}{\rho R}\frac{\partial}{\partial X_j}\left\{2\mu\left(e_{ij} - \tfrac{1}{3}\Delta\delta_{ij}\right)\right\}, \qquad i = 1,2,3, \tag{2.5}$$

$$\frac{\mathrm{D}\rho}{\mathrm{D}t} + \rho\frac{\partial U_j}{\partial X_j} = 0, \tag{2.6}$$

and

$$\rho\frac{\mathrm{D}T}{\mathrm{D}t} - \frac{\gamma-1}{\gamma}\frac{\mathrm{D}p}{\mathrm{D}t} = \frac{M^2(\gamma-1)}{R}\mu\Phi_v + \frac{1}{R\sigma_0}\frac{\partial}{\partial X_j}\left(\mu\frac{\partial T}{\partial X_j}\right), \tag{2.7}$$

where, in these equations,

$$(X_1, X_2, X_3) = (x, y, z); \quad (U_1, U_2, U_3) = (u, v, w), \tag{2.8}$$

$$\frac{\mathrm{D}}{\mathrm{D}t} = \frac{\partial}{\partial t} + U_j \frac{\partial}{\partial X_j}, \tag{2.9}$$

$$e_{ij} = \frac{1}{2}\left(\frac{\partial U_i}{\partial X_j} + \frac{\partial U_j}{\partial X_i}\right), \tag{2.10}$$

$$\Delta = e_{ii}, \tag{2.11}$$

δ_{ij} is the Kronecker delta, Φ_v is the viscous dissipation function and repeated indices imply summation.

The Prandtl number σ_0 is a true parameter of the problem and cannot be scaled out of the governing equations. In this paper we will set $\sigma_0 \equiv 1$. This results in a significant reduction in the still formidable algebra that must be carried out and serves as a rough approximation to the value for air of 0.72. We suppose that the normalized viscosity depends only on the temperature T and carry a general viscosity law $\mu = \mu(T)$ through the analysis, considering a specific form when numerical calculations are carried out.

Our interest is in the spatial development of a pair of oblique (with respect to the free stream direction) instability waves with equal amplitude, frequency and streamwise wavenumber and equal but opposite spanwise wavenumbers. The pair thus forms a standing wave in the spanwise direction that propagates and grows in the streamwise direction. In order to analyse the situation usually encountered in experiments and numerical simulations, we suppose that the disturbance originates from a low-amplitude time-harmonic excitation at a frequency, say ω, near the peak in the linear growth rate curve. The normalized frequency, or Strouhal number, is defined as

$$S \equiv \frac{\omega\delta}{U_\infty}. \tag{2.12}$$

Downstream of the excitation the disturbance will grow according to linear theory. The slow viscous spreading of the mean flow causes the local normalized frequency and spanwise wavenumber of the disturbance to increase as it propagates downstream. This results in a reduction of the local growth rate while the normalized streamwise wavenumber adjusts itself so that the obliqueness angle remains essentially constant. Once mean flow spreading has driven the disturbance close enough to its neutral stability point nonlinear effects will become important within the critical layer while the local amplitude is still relatively small. The linear neutral Strouhal number, streamwise wavenumber and spanwise wavenumber of the instability waves are denoted by S_0, α and $\pm\beta$, respectively. We define $\bar{\alpha}^2 = \alpha^2 + \beta^2$ and denote by $\theta = \tan^{-1}\beta/\alpha$ the angle the instability wave makes with the streamwise direction.

As in GC and WLC nonlinear effects first become important in the critical layer when the local Strouhal number S differs from the linear neutral value by an amount of order $\epsilon^{1/3}$, where $\epsilon \ll 1$ is the order of magnitude of the disturbance amplitude, so that

$$S = S_0 + \epsilon^{1/3} S_1, \tag{2.13}$$

where $S_1 < 0$ is an order-one constant. The spatial growth of the instability wave then occurs over the long lengthscale

$$x_1 = \epsilon^{1/3} x. \tag{2.14}$$

We fix the origin of the x, y, z coordinate system on the surface of the plate at the streamwise position where nonlinear effects first become important.

In order for viscous effects to influence the nonlinear development of the disturbance at leading order we take the scaled viscous parameter

$$\lambda = \frac{1}{\epsilon R} \tag{2.15}$$

to be order one.

2.1. *The solution outside the critical layer*

The flow outside the critical layer is, to the order of accuracy required here, linear in the amplitude of the oblique instability waves and consists of a mean flow that develops on a long (compared with the wavelength) streamwise lengthscale, the near neutral linear disturbances and additional terms which are generated by nonlinear effects within the critical layer.

It is convenient to work in a coordinate moving with the neutral phase speed $U_c = S_0/\alpha$,

$$\xi = x - U_c t. \tag{2.16}$$

The mean flow develops on the viscous lengthscale

$$x_2 = x/R = \epsilon^{2/3}\lambda x_1, \tag{2.17}$$

which is much longer than that over which the near neutral instability waves evolve. It will therefore be sufficient to use the mean flow at the beginning of the nonlinear region, considered as a strictly parallel flow, in this analysis. We denote the mean velocity and temperature profiles at the origin of our streamwise coordinate, $x = 0$, by $U(y) + U_c$ and T_0, respectively.

The solution outside the critical layer expands like

$$u = U(y) + \epsilon^{2/3}a_1(y)x_1 + \epsilon\mathrm{Re}\left\{\sec\theta F(y)A^\dagger(x_1)\mathrm{e}^{\mathrm{i}\alpha\zeta}\cos\beta z + F_1^{(0)}(y)B^\dagger(x_1)\cos 2\beta z\right\} + \epsilon^{4/3}u_2 + \cdots, \tag{2.18}$$

$$v = -\epsilon\left[\mathrm{Re}\left\{\mathrm{i}\bar{\alpha}\Phi(y)A^\dagger(x_1)\mathrm{e}^{\mathrm{i}\alpha\zeta}\cos\beta z\right\} + a_2(y)\right] + \epsilon^{4/3}v_2 + \cdots, \tag{2.19}$$

$$w = -\epsilon\mathrm{Re}\left\{\mathrm{i}\sin\theta\Psi(y)A^\dagger(x_1)\mathrm{e}^{\mathrm{i}\alpha\zeta}\sin\beta z\right\} + \epsilon^{4/3}w_2 + \cdots, \tag{2.20}$$

$$T = T_0(y) + \epsilon^{2/3}a_3(y)x_1 + \epsilon\mathrm{Re}\left\{\Theta(y)A^\dagger(x_1)\mathrm{e}^{\mathrm{i}\alpha\zeta}\cos\beta z + G_1^{(0)}(y)B^\dagger(x_1)\cos 2\beta z\right\} + \epsilon^{4/3}T_2 + \cdots, \tag{2.21}$$

$$p = 1 + \epsilon\gamma M^2\cos\theta\mathrm{Re}\left\{\Pi(y)A^\dagger(x_1)\mathrm{e}^{\mathrm{i}\alpha\zeta}\cos\beta z\right\} + \epsilon^{4/3}p_2 + \epsilon^{5/3}p_3 + \cdots, \tag{2.22}$$

where $\zeta = \xi - S_1\epsilon^{1/3}t/\alpha$ and Re denotes the real part.

The spanwise dependent mean flow distortion term which appears at the same order as the primary instability in (2.18) must be included in the outer expansion to achieve a match with the nonlinear flow in the critical layer as first pointed out by GC. The appearance of this term, as explained by WLC and Goldstein (1994 *a*, *b*), is due to the fact that the leading-order fundamental streamwise and spanwise velocities in (2.18) and (2.20) are algebraically singular at the critical level. This causes the leading-order disturbance velocities in the critical layer to be asymptotically larger than those in the outer region. Nonlinear interactions within the critical layer are then able to produce terms at the same order as the leading terms in the outer region. The amplitude of the mean flow distortion $B^\dagger(x_1)$ is obtained by matching with the critical layer solution and we note that this requires a jump in $F_1^{(0)}$ across this layer.

In the compressible case considered herein the leading-order fundamental disturbance temperature is also singular at the critical level (Reshotko 1960; Lees & Reshotko 1962) and nonlinear interactions in the critical layer induce a spanwise-dependent mean temperature distortion at order ϵ in the same way as for the streamwise velocity. Matching with the critical layer solution similarly requires a jump in $G_1^{(0)}$ across the critical layer. Additional mean flow distortion terms and higher harmonics generated by critical layer nonlinearity are of higher order in the outer region.

The functions $a_1(y), a_2(y)$ and $a_3(y)$ account for the viscous spreading of the mean flow and can be determined by the boundary layer equations but their explicit evaluation is not required to obtain the results of interest here.

The primary goal of the analysis is to determine the amplitude $A^\dagger$ as a function of the long streamwise variable x_1. Since we are interested in the case where nonlinear effects arise due to continued downstream growth of an initially linear disturbance we will require that

$$A^\dagger \to a^\dagger e^{-S_1 U_c' \bar{\kappa} x_1/2} \quad \text{as } x_1 \to -\infty, \tag{2.23}$$

where $a^\dagger$ is a complex constant, $-S_1 U_c' \mathrm{Re}\bar{\kappa}/2$ is the scaled linear growth rate, the prime denotes differentiation with respect to y and the subscript c indicates the function value at the critical point.

For the linear instability of compressible shear flows it is convenient to work with the pressure as the primary dependent variable and obtain the remaining flow variables in their turn. Substituting (2.16)–(2.22) into the governing equations (2.5)–(2.11) and further expanding the primary fundamental linear disturbance quantities about their neutral eigensolutions as

$$\Pi(y) = \Pi_1(y) + \epsilon^{1/3}\Pi_2(y) + \cdots, \tag{2.24}$$

shows that the function $\Pi_1(y)$ satisfies

$$\mathrm{L}\Pi_1 = 0, \tag{2.25}$$

where

$$\mathrm{L} = \frac{1}{T_0}\frac{\mathrm{d}}{\mathrm{d}y}T_0\frac{\mathrm{d}}{\mathrm{d}y} - \frac{2U'}{U}\frac{\mathrm{d}}{\mathrm{d}y} - \bar{\alpha}^2\left(1 - \frac{U^2M^2}{T_0}\cos^2\theta\right) \tag{2.26}$$

is the linear compressible Rayleigh operator, subject to the boundary conditions

$$\Pi_1 \sim a\exp(-\bar{\alpha}(1-(1-U_c)^2M^2\cos^2\theta)^{1/2}y) \quad \text{as } y \to \infty, \tag{2.27}$$

and

$$\Pi_1' = 0 \quad \text{at } y = 0, \tag{2.28}$$

where a is an arbitrary constant.

The Rayleigh problem (2.25)–(2.28) in general requires a numerical solution. However, for purposes of calculating the velocity jump across the critical layer, it is sufficient to obtain the solution in the vicinity of the critical point y_c where $U(y_c) = 0$. In this paper we restrict our attention to the first mode waves classified by Lees & Lin (1946) as 'subsonic' because they have phase speeds relative to the free stream less than the local speed of sound. These modes are exponentially decaying in the free stream and have their critical point coincident with a mean flow generalized inflection point i.e. $U_c''/U_c' = T_c'/T_c$. Letting $\eta = y - y_c$ two linearly independent solutions to (2.25)–(2.26) near $\eta = 0$ can be obtained in a standard way by the method of Frobenius as

$$\tilde{\Pi}^{(1)} = 1 - \tfrac{1}{2}\bar{\alpha}^2\eta^2 + a_4\eta^4 + \cdots, \tag{2.29}$$

and

$$\tilde{\Pi}^{(2)} = \eta^3 - \frac{3}{10}\left[\frac{T_c''}{T_c} - \left(\frac{T_c'}{T_c}\right)^2 + \frac{1}{2}\left(\frac{U_c''}{U_c'}\right)^2 - \frac{2}{3}\frac{U_c'''}{U_c'} - \tfrac{1}{3}\bar{\alpha}^2\right]\eta^5 + \cdots \tag{2.30}$$

as $\eta \to 0$ where

$$a_4 = \tfrac{1}{4}\bar{\alpha}^2\left[\frac{T_c''}{T_c} - \frac{2}{3}\frac{U_c'''}{U_c'} - \left(\frac{T_c'}{T_c}\right)^2 + \frac{1}{2}\left(\frac{U_c''}{U_c'}\right)^2 - \tfrac{1}{2}\bar{\alpha}^2 - \frac{U_c'^2 M^2\cos^2\theta}{T_c}\right]. \tag{2.31}$$

The general solution to (2.25)–(2.28) can then be written as

$$\Pi_1 = \frac{U_c'}{T_c}\left[\tilde{\Pi}^{(1)} + \tfrac{1}{3}\bar{\alpha}^2\left\{b_1 + \frac{1}{2}\frac{U_c''}{U_c'}\right\}\tilde{\Pi}^{(2)}\right], \tag{2.32}$$

where b_1 is a constant determined by the boundary conditions. Having the solution for the pressure we can substitute it into the momentum and energy equations to obtain the leading-order solutions for the disturbance velocity components and temperature near the critical level as

$$F_1 \to \frac{\sin^2\theta}{\eta} + \sin^2\theta\left(\frac{T_c'}{T_c} - \frac{1}{2}\frac{U_c''}{U_c'}\right) - b_1 - \left[\frac{U_c''}{U_c'}b_1 + \frac{1}{2}\left(\frac{U_c''}{U_c'}\right)^2 - \frac{1}{3}\frac{U_c'''}{U_c'} - \tfrac{1}{2}\alpha^2 + \frac{4a_4}{\bar{\alpha}^2}\right.$$
$$\left. - \sin^2\theta\left\{\frac{1}{4}\left(\frac{U_c''}{U_c'}\right)^2 - \frac{1}{6}\frac{U_c'''}{U_c'} - \frac{1}{2}\frac{T_c'}{T_c}\frac{U_c''}{U_c'} + \frac{1}{2}\frac{T_c''}{T_c}\right\}\right]\eta + \cdots, \tag{2.33}$$

$$\Phi_1 \to 1 - b_1\eta + \cdots, \tag{2.34}$$

$$\Psi_1 \to \frac{1}{\eta} + \left(\frac{T_c'}{T_c} - \frac{1}{2}\frac{U_c''}{U_c'}\right) - \left\{\tfrac{1}{2}\bar{\alpha}^2 + \frac{1}{6}\frac{U_c'''}{U_c'} - \frac{1}{4}\left(\frac{U_c''}{U_c'}\right)^2 + \frac{1}{2}\frac{T_c'U_c''}{T_cU_c'} - \frac{1}{2}\frac{T_c''}{T_c}\right\}\eta + \cdots, \tag{2.35}$$

and

$$\Theta_1 \to \frac{T_c'}{U_c'\cos\theta}\left[\frac{1}{\eta} - \left\{b_1 - \frac{T_c''}{T_c'} + \frac{1}{2}\frac{U_c''}{U_c'}\right\}\right] + (\gamma - 1)M^2U_c'\cos\theta + \cdots, \tag{2.36}$$

as $\eta \to 0^{\pm}$.

The correction to the linear neutral eigensolution for the pressure is governed by an inhomogeneous Rayleigh equation whose general solution can be written as

$$A^{\dagger}\Pi_2 = \frac{2iU_c'}{T_c\alpha}\left(U_c\frac{dA^{\dagger}}{dx_1} - iS_1A^{\dagger}\right)\tilde{\Pi}_{P,1} - 2i\alpha\frac{U_c'}{T_c}\frac{dA^{\dagger}}{dx_1}\tilde{\Pi}_{P,2}, \tag{2.37}$$

where

$$\tilde{\Pi}_{P,1} = \Pi_{P,1} + c_{2,1}\tilde{\Pi}^{(1)} + \tfrac{1}{3}\bar{\alpha}^2\left(b_{2,1}^{\pm} + \tfrac{1}{2}\frac{U_c''}{U_c'}\right)\tilde{\Pi}^{(2)}, \tag{2.38}$$

$$\tilde{\Pi}_{P,2} = \Pi_{P,2} + c_{2,2}\tilde{\Pi}^{(1)} + \tfrac{1}{3}\bar{\alpha}^2\left(b_{2,2}^{\pm} + \tfrac{1}{2}\frac{U_c''}{U_c'}\right)\tilde{\Pi}^{(2)}, \tag{2.39}$$

$b_{2,n}^{\pm}$ and $c_{2,n}$ are constants, and $\Pi_{P,1}$ and $\Pi_{P,2}$ are particular solutions of

$$L\Pi_{P,1} = \frac{T_c}{U_c'}\left[\frac{U'}{U^2}\frac{d}{dy} + \frac{U}{T_0}(M\alpha)^2\right]\Pi_1, \tag{2.40}$$

and

$$\mathrm{L}\Pi_{P,2} = \frac{T_c}{U_c'}\left[1 - \frac{(MU)^2}{T_0}\right]\Pi_1, \tag{2.41}$$

subject to the same boundary conditions as those imposed on Π_1. The general solutions to the inhomogeneous Rayleigh problems (2.40) and (2.41) can be obtained by using the neutral eigensolution and the method of variation of parameters as

$$\tilde{\Pi}_{P,1} \to c_{2,1} + \frac{\bar{\alpha}^2}{2U_c'}\eta - \left[\frac{\bar{\alpha}^2}{2U_c'}\left(b_1 + \frac{U_c''}{2U_c'}\right) + \tfrac{1}{2}\bar{\alpha}^2 c_{2,1}\right]\eta^2 + c_{3,L}\eta^3 \ln|\eta| + \left[c_3 + \tfrac{1}{3}\bar{\alpha}^2\left(b_{2,1}^{\pm} + \frac{U_c''}{2U_c'}\right)\right]\eta^3 + \cdots, \tag{2.42}$$

$$\tilde{\Pi}_{P,2} \to c_{2,2} - \tfrac{1}{2}\left(1 + c_{2,2}\bar{\alpha}^2\right)\eta^2 + \tfrac{1}{3}\bar{\alpha}^2\left(b_{2,2}^{\pm} + \frac{U_c''}{2U_c'}\right)\eta^3 + \cdots, \tag{2.43}$$

as $\eta \to 0^{\pm}$, where $c_{3,L}$ and c_3 are constants with the same values above and below the critical layer whose explicit evaluation is not needed to determine the velocity jump across the critical layer. The latter is obtained from the behaviour near the critical level of the correction to the neutral solution for the streamwise velocity which can be written as

$$A^{\dagger}F_2 \to \frac{\mathrm{i}\sin^2\theta}{\alpha U_c'}\frac{1}{\eta^2}\left(U_c\frac{\mathrm{d}A^{\dagger}}{\mathrm{d}x_1} - \mathrm{i}S_1A^{\dagger}\right) + \frac{e_0(x_1)}{\eta} + e_1(x_1)\ln|\eta| + e_2(x_1) + 2\mathrm{i}\alpha\left(b_{2,2}^{\pm} - \frac{1}{\alpha^2}b_1\right)\frac{\mathrm{d}A^{\dagger}}{\mathrm{d}x_1} - \frac{2\mathrm{i}}{\alpha}\left(b_{2,1}^{\pm} - \frac{U_c''}{2U_c'^2}b_1\right)\left(U_c\frac{\mathrm{d}A^{\dagger}}{\mathrm{d}x_1} - \mathrm{i}S_1A^{\dagger}\right) + \tag{2.44}$$

as $\eta \to 0^{\pm}$. The functions e_0, e_1 and e_2 depend only on the slow variable x_1 and are continuous across the critical layer.

Expressions for the jumps $b_{2,1}^{+} - b_{2,1}^{-}$ and $b_{2,2}^{+} - b_{2,2}^{-}$ can be obtained from the first- and second-order problems for the disturbance pressure as follows. The homogeneous Rayleigh equation can be written as

$$\bar{\mathrm{L}}\Pi_1 = \frac{\mathrm{d}}{\mathrm{d}y}\left[\frac{T_0}{U^2}\frac{\mathrm{d}\Pi_1}{\mathrm{d}y}\right] - \frac{\bar{\alpha}^2 T_0}{U^2}\left(1 - \frac{U^2M^2\cos^2\theta}{T_0}\right)\Pi_1 = 0. \tag{2.45}$$

It follows from this and (2.38)–(2.41) that

$$\Pi_1\,\bar{\mathrm{L}}\tilde{\Pi}_{P,1} - \tilde{\Pi}_{P,1}\,\bar{\mathrm{L}}\Pi_1 = \frac{\mathrm{d}}{\mathrm{d}y}\left[\frac{T_0}{U^2}\left(\Pi_1\tilde{\Pi}_{P,1}' - \tilde{\Pi}_{P,1}\Pi_1'\right)\right] = \frac{T_c}{U_c'}\left[\frac{T_0U'}{U^4}\Pi_1'\Pi_1 + \frac{\bar{\alpha}^2M^2\cos^2\theta}{U}\Pi_1^2\right], \tag{2.46}$$

and

$$\Pi_1\,\bar{\mathrm{L}}\tilde{\Pi}_{P,2} - \tilde{\Pi}_{P,2}\,\bar{\mathrm{L}}\Pi_1 = \frac{\mathrm{d}}{\mathrm{d}y}\left[\frac{T_0}{U^2}\left(\Pi_1\tilde{\Pi}_{P,2}' - \tilde{\Pi}_{P,2}\Pi_1'\right)\right] = \frac{T_c}{U_c'}\left(\frac{T_0}{U^2} - M^2\right)\Pi_1^2. \tag{2.47}$$

Terms more singular than $1/\eta$ at the critical level are then eliminated from the right-hand sides of (2.46) and (2.47) (either by using (2.45) or by subtracting terms with the

appropriate singularities) and the result integrated across the boundary layer, with the critical layer excluded. After using (2.29)–(2.32), (2.42) and (2.43) the expressions for the jumps are obtained as

$$b_{2,1}^{+} - b_{2,1}^{-} = -\frac{T_c}{\bar{\alpha}^2} \fint_0^\infty \left\{ \frac{T_0}{U^3} \left(\Pi_1'^2 + \bar{\alpha}^2 \Pi_1^2 \right) + \frac{\bar{\alpha}^2}{U_c'} \frac{T_0}{U^2} \Pi_1 \left[\frac{1}{2} \left(\frac{T_0'}{T_0} - \frac{2U'}{U} \right) \Pi_1 \right.\right.$$
$$\left. + \left(1 - \frac{U^2 M^2 \cos^2 \theta}{T_0} \right) \Pi_1' \right] + \frac{\bar{\alpha}^2}{U_c'^2} \left(\frac{T_c'}{2T_c} - \frac{U_c''}{U_c'} \right) \frac{\mathrm{d}}{\mathrm{d}y} \left(\frac{\Pi_1^2 T_0}{U} \right) \Bigg\} \mathrm{d}y$$
$$- \frac{T_c T_0(0)}{U_c' U_c^2} \Pi_1^2(0) \left[\frac{1}{2} \left(1 - \frac{U_c^2 M^2 \cos^2 \theta}{T_0(0)} \right) - \frac{U_c}{U_c'} \left(\frac{1}{2} \frac{T_c'}{T_c} - \frac{U_c''}{U_c'} \right) \right], \quad (2.48)$$

and

$$b_{2,2}^{+} - b_{2,2}^{-} = \frac{T_c}{\bar{\alpha}^2} \fint_0^\infty \left\{ M^2 \sin^2 \theta \Pi_1^2 + \frac{T_0}{\bar{\alpha}^2 U^2} \Pi_1'^2 \right\} \mathrm{d}y, \quad (2.49)$$

where $\fint$ denotes the Cauchy principal value integral.

It follows from (2.18) and (2.21) that spanwise-dependent mean components must be included in the expansions for the transverse and spanwise velocities at order $\epsilon^{4/3}$ and for the pressure at order $\epsilon^{5/3}$ namely,

$$v_2 = \mathrm{Re} \Phi_2^{(0)}(y) B_{x_1}^{\dagger} \cos 2\beta z + \cdots, \quad (2.50)$$

$$w_2 = \mathrm{Re} \Psi_2^{(0)}(y) B_{x_1}^{\dagger} \sin 2\beta z + \cdots, \quad (2.51)$$

and

$$p_3 = \mathrm{Re} \Pi_3^{(0)}(y) B_{x_1 x_1}^{\dagger} \cos 2\beta z + \cdots. \quad (2.52)$$

Substituting these into the linearized compressible flow equations shows that the mean streamwise velocity and temperature distortions are given by

$$F_1^{(0)} = -\frac{U'}{U + U_c} \Phi_2^{(0)}, \quad (2.53)$$

and

$$G_1^{(0)} = -\frac{T_0'}{U + U_c} \Phi_2^{(0)}, \quad (2.54)$$

respectively, where $\Phi_2^{(0)}(y)$ satisfies the 'steady' compressible Rayleigh equation in terms of the transverse velocity

$$\frac{\mathrm{d}^2 \Phi_2^{(0)}}{\mathrm{d}y^2} - \frac{T_0'}{T_0} \frac{\mathrm{d}\Phi_2^{(0)}}{\mathrm{d}y} + \left(\frac{U' T_0'}{T_0 (U + U_c)} - \frac{U''}{U + U_c} - 4\beta^2 \right) \Phi_2^{(0)} = 0, \quad (2.55)$$

and must match with the critical layer solution as well as satisfy the boundary conditions

$$\Phi_2^{(0)} \sim \mathrm{e}^{-2\beta y} \qquad \text{as } y \to \infty, \quad (2.56)$$

and

$$\Phi_2^{(0)} = 0 \qquad \text{at } y = 0. \quad (2.57)$$

3. The critical layer

The nonlinear non-equilibrium critical layer has thickness of the order of the instability wave growth and so the appropriate scaled transverse coordinate within

this inner region is

$$Y = \frac{y - y_c}{\epsilon^{1/3}} = O(1), \tag{3.1}$$

and the inner limit of the outer solution (which is given in Appendix A) suggests that the flow in the critical layer expands as

$$u = \epsilon^{1/3} U_c' Y + \epsilon^{2/3}\tilde{u}_1 + \epsilon\tilde{u}_2 + \epsilon^{4/3}\tilde{u}_3 + \cdots, \tag{3.2}$$

$$v = \epsilon\tilde{v}_1 + \epsilon^{4/3}\tilde{v}_2 + \cdots, \tag{3.3}$$

$$w = \epsilon^{2/3}\tilde{w}_1 + \epsilon\tilde{w}_2 + \epsilon^{4/3}\tilde{w}_3 + \cdots, \tag{3.4}$$

$$p = 1 + \epsilon\tilde{p}_1 + \epsilon^{4/3}\tilde{p}_2 + \epsilon^{5/3}\tilde{p}_3 \cdots, \tag{3.5}$$

$$T = T_c + \epsilon^{1/3} T_c' Y + \epsilon^{2/3}\tilde{T}_1 + \epsilon\tilde{T}_2 + \cdots. \tag{3.6}$$

The expansion for the viscosity within the critical layer can be obtained from (3.6) by Taylor expansion to find

$$\mu = \mu_c + \epsilon^{1/3}\mu_c' T_c' Y + \epsilon^{2/3}\left[\mu_c'\tilde{T}_1 + \tfrac{1}{2}\mu_c'' T_c'^2 Y^2\right] + \epsilon\left[\mu_c'\tilde{T}_2 + \mu_c'' T_c' Y\tilde{T}_1 + \tfrac{1}{6}\mu_c''' T_c'^3 Y^3\right] + \cdots, \tag{3.7}$$

where the primes on μ_c denote derivatives with respect to T.

To the required order of approximation, the momentum equations in the critical layer are

$$\frac{\mathrm{D}\boldsymbol{u}}{\mathrm{D}t} = -\frac{1}{\gamma M^2 T}\left\{\frac{\partial p}{\partial\zeta} + \epsilon^{1/3}\frac{\partial p}{\partial x_1}, \epsilon^{-1/3}\frac{\partial p}{\partial Y}, \frac{\partial p}{\partial z}\right\} + \lambda\epsilon^{1/3}\frac{\partial}{\partial Y}\left(\mu\frac{\partial \boldsymbol{u}}{\partial Y}\right), \tag{3.8}$$

where

$$\boldsymbol{u} = \{u, v, w\}, \tag{3.9}$$

and in these variables

$$\frac{\mathrm{D}}{\mathrm{D}t} = \frac{\partial}{\partial\zeta} + \epsilon^{1/3}\left[(u + U_c)\frac{\partial}{\partial x_1} - \frac{S_1}{\alpha}\frac{\partial}{\partial\zeta}\right] + \epsilon^{-1/3} v\frac{\partial}{\partial Y} + w\frac{\partial}{\partial z}. \tag{3.10}$$

The energy equation is

$$\frac{\mathrm{D}T}{\mathrm{D}t} = \frac{\gamma - 1}{\gamma} T\frac{\mathrm{D}p}{\mathrm{D}t} + \lambda\epsilon^{1/3}(\gamma - 1)M^2\mu T\left[\left(\frac{\partial u}{\partial Y}\right)^2 + \left(\frac{\partial w}{\partial Y}\right)^2\right] + \lambda\epsilon^{1/3} T\frac{\partial}{\partial Y}\left(\mu\frac{\partial T}{\partial Y}\right), \tag{3.11}$$

and the continuity equation is

$$\left(\frac{\partial}{\partial\zeta} + \epsilon^{1/3}\frac{\partial}{\partial x_1}\right)u + \epsilon^{-1/3}\frac{\partial v}{\partial Y} + \frac{\partial w}{\partial z} = -\frac{1}{\gamma}\frac{\mathrm{D}p}{\mathrm{D}t} + \lambda\epsilon^{1/3}(\gamma - 1)M^2\mu\left[\left(\frac{\partial u}{\partial Y}\right)^2 + \left(\frac{\partial w}{\partial Y}\right)^2\right] + \epsilon^{1/3}\lambda\frac{\partial}{\partial Y}\left(\mu\frac{\partial T}{\partial Y}\right). \tag{3.12}$$

For the purpose of calculating the velocity jump it is convenient to use the spanwise vorticity

$$\begin{aligned}\Omega &= v_\zeta - u_Y \\ &= -U_c' - \epsilon^{1/3}\tilde{u}_{1Y} - \epsilon^{2/3}\tilde{u}_{2Y} + \epsilon\left(\tilde{v}_{1\zeta} - \tilde{u}_{3Y}\right) + \cdots,\end{aligned} \tag{3.13}$$

as a dependent variable in the critical layer which, to the required order of approximation, satisfies

$$\frac{\mathrm{D}\Omega}{\mathrm{D}t} - \Omega\frac{\partial w}{\partial z} - \frac{\Omega}{\gamma p}\frac{\mathrm{D}p}{\mathrm{D}t} = -\lambda\epsilon^{1/3}(\gamma-1)M^2\mu\Omega\left[\left(\frac{\partial u}{\partial Y}\right)^2 + \left(\frac{\partial w}{\partial Y}\right)^2\right]$$
$$-\frac{\lambda\epsilon^{1/3}}{p}\Omega\frac{\partial}{\partial Y}\left(\mu\frac{\partial T}{\partial Y}\right) + \epsilon^{-1/3}\frac{\partial w}{\partial Y}\frac{\partial u}{\partial z} + \frac{\epsilon^{-1/3}}{\gamma M^2}\frac{\partial T}{\partial Y}\left(\frac{\partial p}{\partial \zeta} + \epsilon^{1/3}\frac{\partial p}{\partial x_1}\right)$$
$$+\lambda\epsilon^{1/3}T\mu\frac{\partial^2\Omega}{\partial Y^2} - \lambda\frac{\partial^2 u}{\partial Y^2}\frac{\partial}{\partial Y}(T\mu) - \lambda\frac{\partial}{\partial Y}\left(T\frac{\partial\mu}{\partial Y}\frac{\partial u}{\partial Y}\right). \tag{3.14}$$

Substituting the critical layer expansions (3.2)–(3.7) and (3.13) into (3.8)–(3.12) and (3.14) and equating the lowest-order terms shows that

$$\tilde{v}_1 = -\bar{\alpha}\cos\beta z\,\mathrm{Re}\,\mathrm{i}A^{\dagger}\mathrm{e}^{\mathrm{i}\alpha\zeta} + a_{2c}, \tag{3.15}$$

$$\tilde{p}_1 = \frac{\gamma M^2 U_c'}{T_c}\cos\theta\cos\beta z\,\mathrm{Re}A^{\dagger}\mathrm{e}^{\mathrm{i}\alpha\zeta}, \tag{3.16}$$

$$\mathscr{L}\tilde{u}_1 = \bar{\alpha}U_c'\sin^2\theta\cos\beta z\,\mathrm{Re}\,\mathrm{i}A^{\dagger}\mathrm{e}^{\mathrm{i}\alpha\zeta} + \phi_1, \tag{3.17}$$

$$\mathscr{L}\tilde{w}_1 = \beta U_c'\cos\theta\sin\beta z\,\mathrm{Re}A^{\dagger}\mathrm{e}^{\mathrm{i}\alpha\zeta}, \tag{3.18}$$

$$\mathscr{L}\tilde{T}_1 = \bar{\alpha}T_c'\cos\beta z\,\mathrm{Re}\,\mathrm{i}A^{\dagger}\mathrm{e}^{\mathrm{i}\alpha\zeta} + \tau_1, \tag{3.19}$$

where

$$\mathscr{L} = \left(U_c'Y - \frac{S_1}{\alpha}\right)\frac{\partial}{\partial\zeta} + U_c\frac{\partial}{\partial x_1} - \lambda\mu_c T_c\frac{\partial^2}{\partial Y^2}, \tag{3.20}$$

a_{2c} is the value at the critical level of the function a_2 arising from the slowly varying mean flow and ϕ_1 and τ_1 are constants given in Appendix B. The leading-order disturbance terms in the expansions (3.2)–(3.7) therefore can be seen to have only fundamental and mean flow components.

At the next order we have

$$\mathscr{L}\tilde{u}_{2Y} = -\tilde{v}_1\tilde{u}_{1YY} + (\tilde{u}_1\tilde{w}_{1z} - \tilde{u}_{1z}\tilde{w}_1)_Y + U_c'\left(\tilde{w}_{2z} - Y\tilde{u}_{1Yx_1}\right) + \frac{T_c'}{\gamma M^2}\tilde{p}_{1\zeta} + \mathscr{U}_2, \tag{3.21}$$

$$\mathscr{L}\tilde{w}_2 = -\left[\tilde{u}_1\frac{\partial}{\partial\zeta} + \tilde{v}_1\frac{\partial}{\partial Y} + \tilde{w}_1\frac{\partial}{\partial z}\right]\tilde{w}_1 - \frac{T_c}{\gamma M^2}\tilde{p}_{2z} - \frac{T_c'Y}{\gamma M^2}\tilde{p}_{1z} + \mathscr{W}_2, \tag{3.22}$$

$$\mathscr{L}\tilde{T}_2 = -\left[\tilde{u}_1\frac{\partial}{\partial\zeta} + \tilde{v}_1\frac{\partial}{\partial Y} + \tilde{w}_1\frac{\partial}{\partial z}\right]\tilde{T}_1 - T_c'\tilde{v}_2 + \frac{\gamma-1}{\gamma}\mathscr{L}\tilde{p}_1 + \mathscr{T}_2, \tag{3.23}$$

and

$$\tilde{p}_2 = \gamma M^2\cos\theta\frac{U_c'}{T_c}\cos\beta z\,\mathrm{Re}\left\{\frac{2\mathrm{i}c_{2,1}}{\bar{\alpha}\cos\theta}\left(U_c\frac{\mathrm{d}A^{\dagger}}{\mathrm{d}x_1} - \mathrm{i}S_1A^{\dagger}\right) - 2\mathrm{i}\alpha c_{2,2}\frac{\mathrm{d}A^{\dagger}}{\mathrm{d}x_1}\right\}\mathrm{e}^{\mathrm{i}\alpha\zeta}, \tag{3.24}$$

where $\mathscr{U}_2$, $\mathscr{W}_2$ and $\mathscr{T}_2$ are viscous terms given in Appendix B which do not contribute to the solutions of the harmonic components of interest.

The velocity jump across the critical layer can be obtained by integrating the $O(\epsilon)$ term in the expansion for the spanwise vorticity (3.13). The relevant vorticity equation can be written as

$$\mathscr{L}\tilde{q}_3 = \frac{\partial}{\partial Y}\left[-S_{12} + \frac{\tan\theta}{\alpha\beta}\frac{\partial^2}{\partial\zeta\partial z}S_{32}\right] - \frac{T_c'}{\gamma M^2}\left(\tilde{p}_{2\zeta} + \tilde{p}_{1x_1}\right)$$

$$-\frac{T_c''Y}{\gamma M^2}\tilde{p}_{1\zeta}+\frac{1}{\gamma M^2}\frac{\tan\theta}{\alpha\beta}\left(T_c''Y\tilde{p}_1+T_c'\tilde{p}_2+T_c\tilde{p}_{3Y}\right)_{\zeta zz}$$
$$-\phi_3\cos\beta z\,\mathrm{Re}\left[\mathrm{i}\left(\alpha U_c'Y-S_1\right)A^\dagger+U_c\frac{\mathrm{d}A^\dagger}{\mathrm{d}x_1}\right]\mathrm{e}^{\mathrm{i}\alpha\zeta}, \tag{3.25}$$

where we have put

$$\tilde{q}_3=\tilde{u}_{3Y}-\tilde{v}_{1\zeta}-\frac{U_c'}{\gamma}\tilde{p}_1-\frac{\tan\theta}{\alpha\beta}\tilde{w}_{3\zeta Yz}-\phi_3\cos\beta z\mathrm{Re}A^\dagger\mathrm{e}^{\mathrm{i}\alpha\zeta}, \tag{3.26}$$

$$S_{12}=\frac{\partial}{\partial\zeta}(2\tilde{u}_1\tilde{u}_2)+\frac{\partial}{\partial Y}(\tilde{v}_1\tilde{u}_2+\tilde{v}_2\tilde{u}_1)+\frac{\partial}{\partial z}(\tilde{w}_1\tilde{u}_2+\tilde{w}_2\tilde{u}_1), \tag{3.27}$$

$$S_{32}=\frac{\partial}{\partial\zeta}(\tilde{u}_1\tilde{w}_2+\tilde{u}_2\tilde{w}_1)+\frac{\partial}{\partial Y}(\tilde{v}_1\tilde{w}_2+\tilde{v}_2\tilde{w}_1)+\frac{\partial}{\partial z}(2\tilde{w}_1\tilde{w}_2), \tag{3.28}$$

ϕ_3 is a constant given in Appendix B and we have written only the terms that contribute to the jump in the fundamental component of the streamwise velocity.

It is seen from (3.15)–(3.24) that the nonlinear interaction of the lowest-order fundamental solutions will produce first harmonics and mean flow distortion terms at this order so that the solutions will be of the form

$$\tilde{u}_{2Y}=\tfrac{1}{2}U_c'''Y^2-h_2x_1+\ \mathrm{Re}\ \tilde{U}_{2Y}^{(0,0)}+\ \mathrm{Re}\ \tilde{U}_{2Y}^{(2,0)}\mathrm{e}^{2\mathrm{i}\alpha\zeta}+\cos\beta z\ \mathrm{Re}\ \tilde{U}_{2Y}^{(1,1)}\mathrm{e}^{\mathrm{i}\alpha\zeta}$$
$$+\cos2\beta z\ \mathrm{Re}\ \tilde{U}_{2Y}^{(0,2)}+\cos2\beta z\ \mathrm{Re}\ \tilde{U}_{2Y}^{(2,2)}\mathrm{e}^{2\mathrm{i}\alpha\zeta}, \tag{3.29}$$

$$\tilde{w}_2=\sin\beta z\ \mathrm{Re}\left\{\tilde{W}_2^{(1,1)}-\sin\theta\left(\frac{T_c'}{T_c}-\tfrac{1}{2}\frac{U_c''}{U_c'}\right)\mathrm{i}A^\dagger\right\}\mathrm{e}^{\mathrm{i}\alpha\zeta}$$
$$+\sin2\beta z\ \mathrm{Re}\ \tilde{W}_2^{(0,2)}+\sin2\beta z\ \mathrm{Re}\ \tilde{W}_2^{(2,2)}\mathrm{e}^{2\mathrm{i}\alpha\zeta}, \tag{3.30}$$

and

$$\tilde{T}_2=\tfrac{1}{6}T_c'''Y^3+\tau_2Yx_1+\ \mathrm{Re}\ \bar{T}_2^{(0,0)}+\ \mathrm{Re}\ \bar{T}_2^{(2,0)}\mathrm{e}^{2\mathrm{i}\alpha\zeta}+\cos\beta z\ \mathrm{Re}\ \bar{T}_2^{(1,1)}\mathrm{e}^{\mathrm{i}\alpha\zeta}$$
$$+\cos2\beta z\ \mathrm{Re}\ \bar{T}_2^{(0,2)}+\cos2\beta z\ \mathrm{Re}\ \bar{T}_2^{(2,2)}\mathrm{e}^{2\mathrm{i}\alpha\zeta}, \tag{3.31}$$

where h_2 and τ_2 are constants that can be obtained by solving for the corresponding mean components and matching with the outer solution. For purposes of computing the fundamental velocity jump across the critical layer from the next-order solution only the (0, 0) and (0, 2) components of (3.29)–(3.31) need to be obtained and GC further showed that only the complex conjugates of these produce terms that make non-zero contributions to the jump. The relevant solutions for the streamwise and spanwise velocities in the viscous case are given by WLC. The spanwise-dependent mean component $\tilde{U}_2^{(0,2)}$ is responsible for the corresponding component in the outer region due to the fact that it approaches (different) finite values at the upper and lower edges of the critical layer (GC; WLC). Nonlinear interactions of the lowest-order fundamental solutions in the energy equation (3.23) produce mean distortion components of the temperature and it can be shown that

$$\bar{T}_2^{(0,2)}\sim\pm\frac{\pi S_1U_cT_c'}{\alpha}\tan^2\theta\sin^2\theta\int_{-\infty}^{\bar{x}}\int_{-\infty}^{\xi_1}(\bar{x}-\xi_1)\mathrm{e}^{-2\bar{\lambda}(\xi_1-\xi_2)^3/3}|A(\xi_2)|^2\mathrm{d}\xi_2\mathrm{d}\xi_1 \tag{3.32}$$

as $Y\to\pm\infty$ where we have introduced the normalized variables

$$\bar{x}=-\tfrac{1}{2}S_1U_c'x_1-x_0,\quad\bar{\lambda}=\frac{-8\alpha^2T_c\mu_c}{U_c'(S_1U_c)^3}\lambda \tag{3.33}$$

and

$$A = \frac{4\alpha^2}{(S_1 U_c)^2 U_c'} A^\dagger e^{iX_0}. \tag{3.34}$$

Thus nonlinear critical layer effects induce a spanwise-dependent mean distortion of the temperature in the outer region at the same order as the primary disturbance in the compressible case. The outer expansion must therefore include a term that will match on to this and we have included such a term in (2.21). Upon carrying out the matching, and using (2.53) and (2.54), it is found that

$$\Phi_2^{(0)}(y_c^\pm) = \mp \frac{\pi S_1 U_c^2}{\alpha} \tan^2\theta \sin^2\theta, \tag{3.35}$$

and

$$B^\dagger(x_1) \equiv B(\bar{x}) = \int_{-\infty}^{\bar{x}} \int_{-\infty}^{\xi_1} (\bar{x} - \xi_1) e^{-2\bar{\lambda}(\xi_1 - \xi_2)^3/3} |A(\xi_2)|^2 d\xi_2 d\xi_1. \tag{3.36}$$

Equation (3.35) provides the jump condition that must be satisfied by the solution to the steady Rayleigh equation (2.55) while (3.36) gives the streamwise evolution of the amplitude of the mean distortion in terms of the amplitude of the fundamental instability. An equation for the latter is obtained by matching the velocity jump in the outer solution with that calculated from the solution to (3.25). Using (3.26) the matching condition can be written as

$$\cos\theta \int_{-\infty}^{\infty} \tilde{q}_3^{(1,1)} dY = 2i\alpha \left(b_{2,2}^+ - b_{2,2}^-\right) \frac{dA^\dagger}{dx_1} - \frac{2i}{\alpha} \left(b_{2,1}^+ - b_{2,1}^-\right) \left(U_c \frac{dA^\dagger}{dx_1} - iS_1 A^\dagger\right). \tag{3.37}$$

The contributions to the fundamental component of $\tilde{q}_3$, and the velocity jump across the critical layer from the nonlinear terms (3.27) and (3.28) have been given by WLC. Here we have additional linear terms due to the mean temperature derivatives at the critical level. The contributions of these new terms to the velocity jump are easily obtained by the now standard Fourier transform method of Hickernell (1984).

4. The amplitude equation

Upon equating the velocity jumps from the outer linear solution (2.44) and the nonlinear critical layer solution the equation governing the streamwise evolution of the instability wave amplitude can be written as

$$\frac{\bar{\gamma}}{\bar{\kappa}} \frac{dA}{d\bar{x}} = \bar{\gamma} A - \int_{-\infty}^{\bar{x}} \int_{-\infty}^{\xi_1} \mathscr{K} A(\xi_1) A(\xi_2) A^*(\xi_1 + \xi_2 - \bar{x}) d\xi_2 d\xi_1, \tag{4.1}$$

where the kernel function is defined as

$$\begin{aligned} \mathscr{K}(\bar{x}, \xi_1, \xi_2; \theta, \bar{\lambda}) = {} & \exp(-\bar{\lambda}(\bar{x} - \xi_1)^2 [\tfrac{2}{3}(\bar{x} - \xi_1) + (\xi_1 - \xi_2)]) \\ & \times \{\mathscr{K}_I + 2\sin^2\theta \mathscr{K}_{II} + 8\sin^4\theta \mathscr{K}_{III}\}, \end{aligned} \tag{4.2}$$

where

$$\mathscr{K}_I = (\bar{x} - \xi_1)^2 [2(\bar{x} - \xi_1) + (\xi_1 - \xi_2)], \tag{4.3}$$

$$\begin{aligned} \mathscr{K}_{II} = {} & \int_{\xi_2}^{\xi_1} (\bar{x} - \xi_1)[(\bar{x} - \xi_1) + 2(\xi_1 - \xi_3)] \chi_1 d\xi_3 \\ & - \int_{\xi_1}^{\bar{x}} (\bar{x} - \xi_3)[2(\xi_3 - \xi_2) + (\bar{x} - \xi_1) + (\xi_3 - \xi_1)]\{\chi_2 + \chi_3\} d\xi_3 \end{aligned}$$

$$+2\int_{\xi_1}^{\bar{x}}(\xi_1-\xi_2)(\xi_3-\xi_1)[1+2\bar{\lambda}(\bar{x}-\xi_3)(\bar{x}-\xi_2+\xi_3-\xi_1)^2]\chi_4 \mathrm{d}\xi_3, \tag{4.4}$$

$$\begin{aligned}\mathscr{K}_{III} = &-\int_{\xi_1}^{\bar{x}}\int_{\xi_3}^{\xi_2}(\xi_2-\xi_4)[1+2\bar{\lambda}(\bar{x}-\xi_3)(\xi_3-\xi_1)^2]\chi_5 \mathrm{d}\xi_4\mathrm{d}\xi_3\\ &-2\int_{\xi_1}^{\bar{x}}\int_{\xi_3}^{\xi_1}(\xi_4-\xi_1)[1+2\bar{\lambda}(\bar{x}-\xi_3)(\bar{x}-\xi_1+\xi_3-\xi_2)^2]\chi_6 \mathrm{d}\xi_4\mathrm{d}\xi_3\\ &-\int_{\xi_1}^{\bar{x}}\int_{\xi_3}^{\xi_1}(\xi_1-\xi_4)[1+2\bar{\lambda}(\bar{x}-\xi_3)(\xi_3-\xi_2)^2]\chi_7 \mathrm{d}\xi_4\mathrm{d}\xi_3,\end{aligned} \tag{4.5}$$

and the χ_n are exponential functions of $\bar{x}, \xi_1, \xi_2, \xi_3, \xi_4$, and $\bar{\lambda}$ given in Appendix C. The coefficients appearing in the amplitude equation (4.1) are given as

$$\bar{\gamma} = \frac{-2\mathrm{i}U_c S_1^2}{\alpha^2 \tan^2\theta U_c'}\left[\frac{T_c''}{T_c} - \frac{U_c'''}{U_c'} + \frac{2\mathrm{i}U_c'}{\pi}(b_{2,1}^+ - b_{2,1}^-)\right], \tag{4.6}$$

and

$$\frac{\bar{\gamma}}{\bar{\kappa}} = \tfrac{1}{2}\mathrm{i}U_c U_c' \bar{\gamma} - \frac{2\mathrm{i}U_c U_c' S_1^2}{\pi \tan^2\theta}(b_{2,2}^+ - b_{2,2}^-). \tag{4.7}$$

These complex constants are fully determined by combining (4.6) and (4.7) with (2.48), (2.49) and the neutral solution to (2.25)–(2.28). They depend upon the particular mean flow under consideration and the values of the relevant physical parameters.

As shown by GC and WLC the solution to the amplitude equation (4.1) can be completely characterized by the three real parameters arg $(\bar{\kappa}/\bar{\gamma})$, $\hat{\lambda} = \bar{\lambda}/\bar{\kappa}_r^3$ and θ, where the subscript r refers to the real part of a complex quantity, upon introducing the normalized variables

$$\hat{A} = \mathrm{e}^{-\mathrm{i}(\zeta_0 + \bar{\kappa}_i \bar{x})}\frac{|\bar{\kappa}|^{1/2}}{|\bar{\gamma}|^{1/2}\bar{\kappa}_r^3}A, \tag{4.8}$$

and

$$\hat{x} = \bar{\kappa}_r \bar{x} - \bar{x}_0, \tag{4.9}$$

so that (4.1) becomes

$$\frac{\mathrm{d}\hat{A}}{\mathrm{d}\hat{x}} = \hat{A} - \mathrm{e}^{\mathrm{i}\arg(\bar{\kappa}/\bar{\gamma})}\int_{-\infty}^{\hat{x}}\int_{-\infty}^{\xi_1}\mathscr{K}\hat{A}(\xi_1)\hat{A}(\xi_2)\hat{A}^*(\xi_1+\xi_2-\hat{x})\mathrm{d}\xi_2\mathrm{d}\xi_1, \tag{4.10}$$

subject to the upstream boundary condition

$$\hat{A} \to \mathrm{e}^{\hat{x}} \text{ as } \hat{x} \to -\infty, \tag{4.11}$$

when the coordinate shifts are appropriately chosen.

We further introduce

$$\hat{B} = \frac{|\bar{\kappa}|}{|\bar{\gamma}|\bar{\kappa}_r^3}B, \tag{4.12}$$

so that in terms of these normalized variables the amplitude of the spanwise-dependent mean flow distortion is

$$\hat{B} = \int_{-\infty}^{\hat{x}}\int_{-\infty}^{\xi_1}(\hat{x}-\xi_1)\,\mathrm{e}^{-2\hat{\lambda}(\xi_1-\xi_2)^3/3}|\hat{A}(\xi_2)|^2\mathrm{d}\xi_2\mathrm{d}\xi_1. \tag{4.13}$$

The general character of the solutions to (4.10) and (4.11) is now well known. In

the inviscid limit GC showed that the solutions always end in a singularity at a finite downstream position and gave the asymptotic form for the singularity. The viscous solutions, as obtained by WLC, either end in the same singularity or ultimately exhibit exponential decay depending on the values of arg $(\bar{\kappa}/\bar{\gamma})$, θ and $\hat{\lambda}$. The ultimate form of the viscous solutions is suggested by the limiting form of the amplitude equation for large $\hat{\lambda}$ derived by WLC which, in our notation, can be written as

$$\frac{\mathrm{d}\tilde{A}}{\mathrm{d}\tilde{x}} = \hat{\lambda}^{1/3}\tilde{A} - \frac{\bar{g}}{|\bar{g}_r|}\tilde{A}\int_{-\infty}^{\tilde{x}} |\tilde{A}(\xi)|^2 \mathrm{d}\xi, \tag{4.14}$$

where

$$\tilde{A} = \hat{\lambda}^{-1/3}|\bar{g}_r|^{1/2}\hat{A}; \quad \tilde{x} = \hat{\lambda}^{-1/3}\hat{x}, \tag{4.15}$$

and

$$\bar{g} = \cos 2\theta \frac{\bar{\kappa}}{\bar{\gamma}} \frac{|\bar{\gamma}|}{|\bar{\kappa}|} \sin^2\theta \frac{2\Gamma(\frac{1}{3})}{(18)^{1/3}}. \tag{4.16}$$

The analytical solution to this equation obtained by WLC similarly becomes singular or decays exponentially depending on the sign of $\bar{g}_r$. In particular if $\bar{g}_r < 0$ the solution becomes singular while for $\bar{g}_r > 0$ the solution decays exponentially. It might be expected then, as suggested by WLC, that the singularity in the inviscid solutions to (4.10) could be eliminated for sufficiently large (but finite) values of the viscous parameter $\hat{\lambda}$ when $\bar{g}_r > 0$. To confirm this numerical solutions for (4.10) and (4.11) must be obtained. In the next section we present numerical results for the coefficients and the amplitude equation for the first mode instability in a supersonic boundary layer.

5. Numerical results

5.1. *Linear calculations for the coefficients*

Values for the coefficient arg $(\bar{\kappa}/\bar{\gamma})$ appearing in the scaled amplitude equation (4.10) can be obtained from (4.6), (4.7), (2.48), (2.49), and the neutral solution to (2.25)–(2.28). We have computed results for Mach numbers between 2 and 6 for a number of wall heat transfer conditions and obliqueness angles. Mean velocity profiles were obtained by numerical solution of the steady two-dimensional boundary layer equations in the form

$$U + U_c = T_0 f'(\tilde{y}), \tag{5.1}$$

where

$$\tilde{y} = x^{-1/2}y, \tag{5.2}$$

and f satisfies

$$\left[\mu\left(T_0 f'\right)'\right]' + \tfrac{1}{2} f\left(T_0 f'\right)' = 0, \tag{5.3}$$

with

$$f' \to 1 \text{ as } \tilde{y} \to \infty; \quad f = f' = 0 \text{ at } \tilde{y} = 0. \tag{5.4}$$

The Sutherland viscosity law

$$\mu = \frac{T_0^{3/2}}{\frac{1}{2} + T_0} \tag{5.5}$$

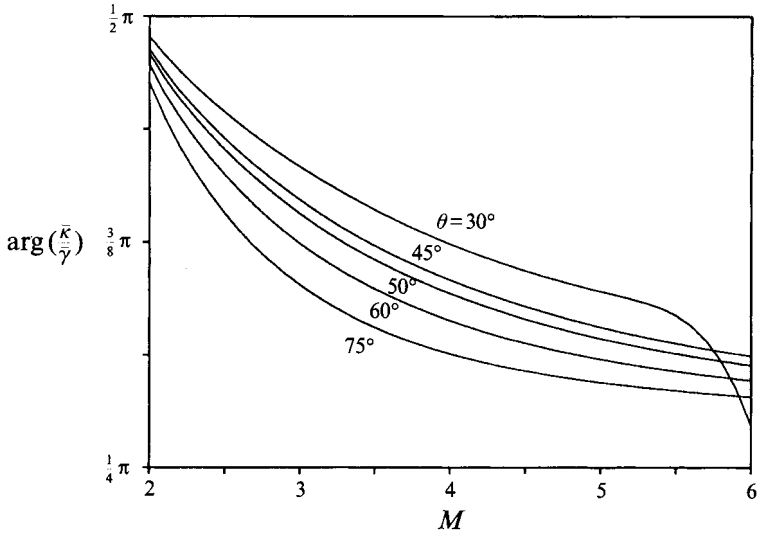

FIGURE 1. Plot of arg $(\bar{\kappa}/\bar{\gamma})$ *vs.* Mach number for an insulated wall at various obliqueness angles.

is used to relate the viscosity to the temperature and the Crocco–Bussman relation gives the latter as

$$T_0 = t_b + (1 - t_b)(U + U_c) + \tfrac{1}{2}(\gamma - 1)M^2(t_b + U + U_c)(1 - U - U_c), \qquad (5.6)$$

where t_b is related to the wall temperature. The insulated wall case corresponds to $t_b = 1$ and a cooled wall to $t_b < 1$.

Figure 1 shows arg $(\bar{\kappa}/\bar{\gamma})$ *vs.* Mach number for an insulated wall and various obliqueness angles. Over this Mach number range the most rapidly growing first mode waves have $50° < \theta < 70°$ (Mack 1984). For these angles the results in figure 1, along with (4.16), show that, over the entire Mach number range for which the theory is expected to apply, the coefficient falls within the range where the viscous limit equation derived by WLC develops a singularity. The results show that arg $(\bar{\kappa}/\bar{\gamma})$ decreases away from $\pi/2$ as the Mach number increases until it appears to become independent of M beyond about 6 for the most rapidly growing waves. It is also seen that smaller obliqueness angles correspond to values of arg $(\bar{\kappa}/\bar{\gamma})$ closer to $\pi/2$.

In figure 2 the effect of wall cooling on arg $(\bar{\kappa}/\bar{\gamma})$ for $\theta = 60°$ is shown over the same Mach number range. It shows that, for a fixed wave angle, wall cooling causes arg $(\bar{\kappa}/\bar{\gamma})$ to move closer to $\pi/2$ relative to the insulated case. For the more highly cooled cases arg $(\bar{\kappa}/\bar{\gamma})$ begins to move fairly quickly toward $\pi/2$ as the Mach number decreases from 6 but before it can reach there the generalized inflection point vanishes and the first mode instability no longer exists.

It was shown by GC that when $\theta = 45°$ the nonlinear term vanishes in the inviscid limit while WLC showed that the same is true for their viscous limit equation. It is only for finite values of $\hat{\lambda}$ that the nonlinear term is non-zero when $\theta = 45°$. Furthermore, (4.16) shows that $\bar{g}_r$ changes sign as θ goes through 45°, provided that Re $(\bar{\kappa}/\bar{\gamma})$ does not also change sign. This angle therefore serves as a sort of demarcation between the singular and decaying solutions – at least in the highly viscous limit.

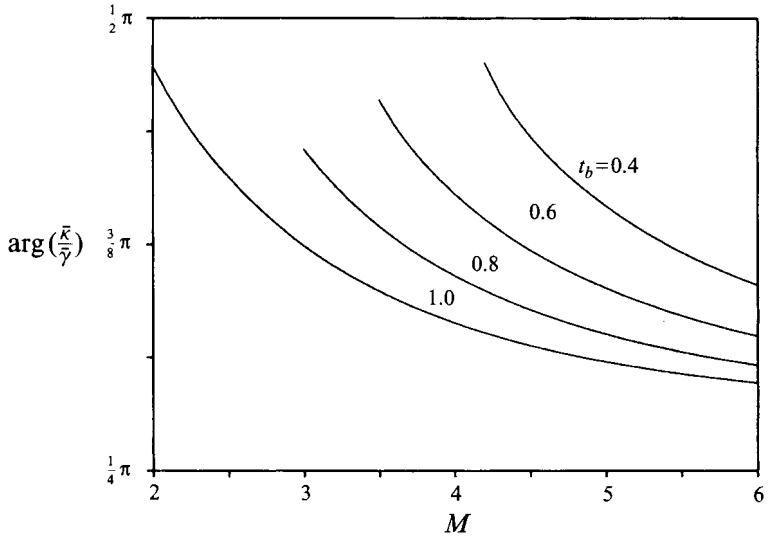

FIGURE 2. Plot of arg $(\bar{\kappa}/\bar{\gamma})$ *vs.* Mach number for $\theta = 60°$ and various amounts of wall cooling.

We have found no cases for the first mode instability where $\bar{g}_r > 0$ for angles corresponding to the most rapidly growing waves. However, as pointed out by WLC, since the coefficient $\bar{g}$ in their viscous limit equation depends on θ, it is always possible to find some angle for which its solution exhibits exponential decay. Returning to figure 1 it is seen that, for example, waves at $\theta = 30°$ will decay in this limit. In fact these results, along with (4.16), suggest that all first mode waves with $\theta < 45°$ will decay in the viscous limit, although these are not the most rapidly growing waves (Mack 1984).

The results from the linear neutral stability calculations presented above, together with the solution to the viscous limit equation of WLC, suggest that in the case of a supersonic boundary layer oblique wave critical layer interaction augments the growth of the most rapidly growing modes and can suppress (for large enough viscosity) the much more slowly growing waves with smaller obliqueness angles. Numerical solutions for the amplitude equation are needed to confirm these conjectures and we present these in the next subsection.

5.2. *Numerical solution of the amplitude equation*

Numerical solutions to the amplitude equation were obtained using the computed values for the coefficients presented above. The computer code was adapted from that used by Goldstein & Lee (1992) in their resonant triad analysis. The solution is advanced downstream from the prescribed linear solution by a variable (up to twelfth)-order Adams–Moulton method. Integrals are computed using the (up to eleventh-order) Newton–Cotes formula.

Solutions for the inviscid case ($\hat{\lambda} = 0$) are shown in figures 3–5. They all end in a singularity whose form was first given by GC and the results show how the singularity position, which can only be found by numerical solution of (4.10), is affected by the physical parameters. In figure 3 the inviscid amplitude evolution is shown for an insulated wall with $\theta = 60°$ at three Mach numbers. The curves show that increasing the Mach number causes the singularity position to move upstream

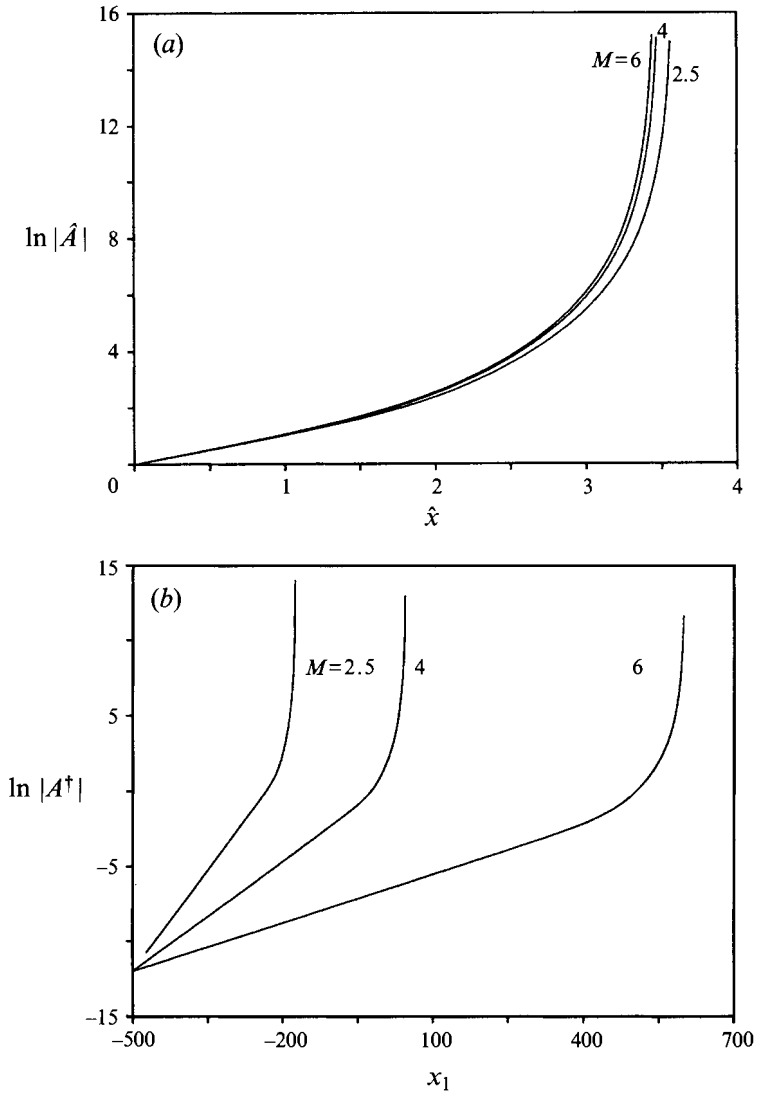

FIGURE 3. Inviscid solution for amplitude *vs.* streamwise position for an insulated wall with $\theta = 60°$ at three different Mach numbers: (*a*) normalized variables and (*b*) physical variables.

in the normalized variables. Part (*b*) of this figure shows that the results look quite different when plotted in the original physical variables (i.e. those appearing in the expansions (2.18)–(2.22) before the various normalizations are introduced). The larger linear growth rate at lower Mach numbers, which is scaled out of the results in figure 3(*a*), causes the singularity to appear further upstream when the disturbances are initiated at equal amplitude in the linear region. The effect of wall cooling on the singularity is shown in figure 4 for $M = 4$ and $\theta = 60°$. It is seen that cooling the wall delays the appearance of the singularity relative to the insulated case by decreasing the linear growth rate. The singularity position in normalized variables in the inviscid case appears to be most sensitive to the wave angle as figure 5 shows. This may be because the kernel function itself, as well as the coefficient in (4.10), depends upon

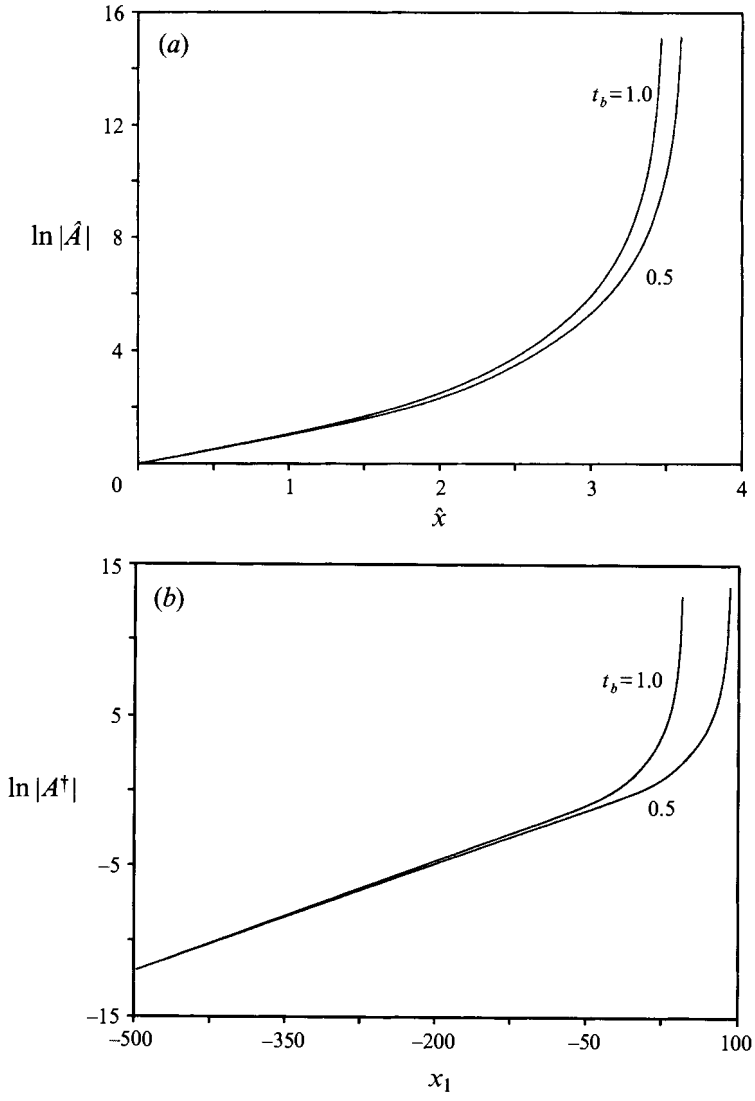

FIGURE 4. Inviscid solution for amplitude *vs.* streamwise position at $M = 4$ and $\theta = 60°$ for an insulated and cooled wall: (*a*) normalized variables and (*b*) physical variables.

θ. Decreasing the obliqueness angle moves the singularity position downstream in normalized variables but figure 5(*b*) shows that the position in physical variables moves upstream. The latter occurs because the near neutral growth rate is larger for the smaller obliqueness angles shown in the figure.

None of the inviscid solutions presented above exhibit any oscillations on their approach to the singularity. This is because of the values of the coefficient arg $(\bar{\kappa}/\bar{\gamma})$ found to be relevant to the supersonic boundary layer. For this flow then the periodic energy transfer between the disturbances and the mean flow associated with these oscillations is absent. Previous weakly nonlinear critical layer calculations, such as those carried out by GC, Goldstein & Leib (1989), Leib (1991), Goldstein & Lee (1992)

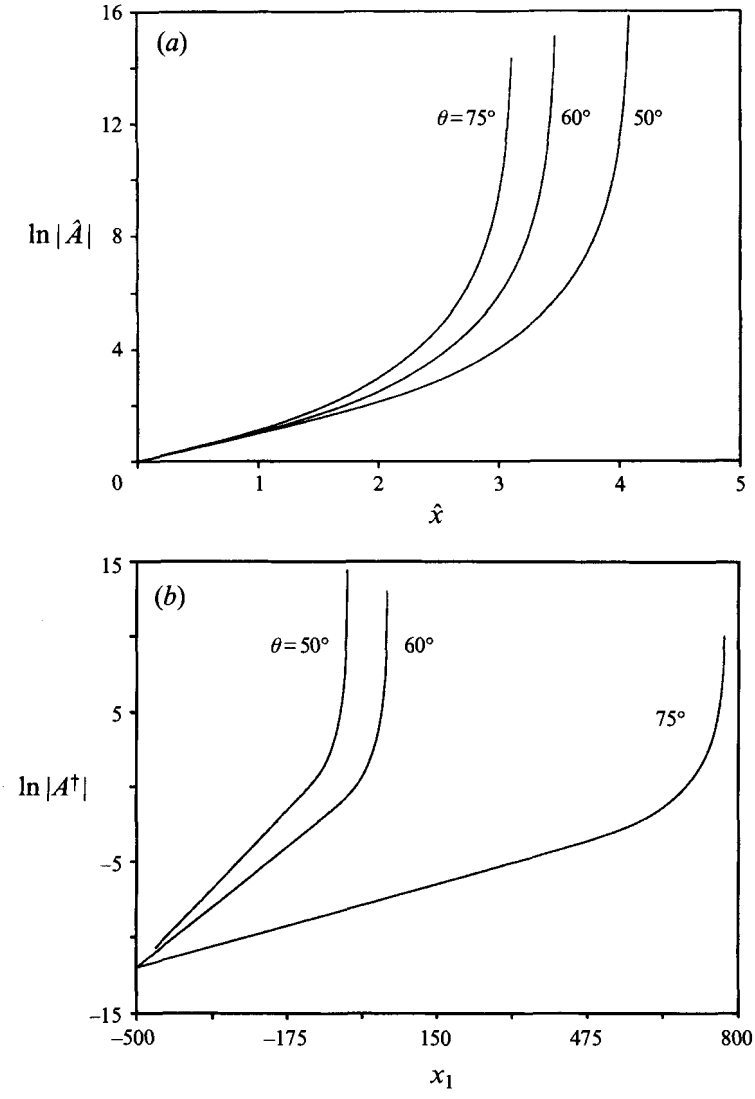

FIGURE 5. Inviscid solution for amplitude *vs.* streamwise position for an insulated wall at $M = 4$ for various obliqueness angles: (*a*) normalized variables and (*b*) physical variables.

and WLC, have shown that in these cases the solution is well approximated by the local asymptotic singularity solution over most of its evolution.

As already discussed, the values of the coefficient in (4.10) for the most rapidly growing first mode waves in a supersonic boundary layer are such that viscous effects are not expected to be able to eliminate the singularity that develops in the inviscid solutions just described. The results of WLC, as well as those from other weakly nonlinear critical layer calculations, show that in such cases viscosity can only delay the occurrence of the singularity. This is accomplished mainly by extending the distance over which the amplitude exhibits linear growth.

Numerical solutions for the amplitude equation corresponding to $M = 4, \theta = 60°$ and an insulated wall are shown in figure 6(*a*) for various values of the viscous

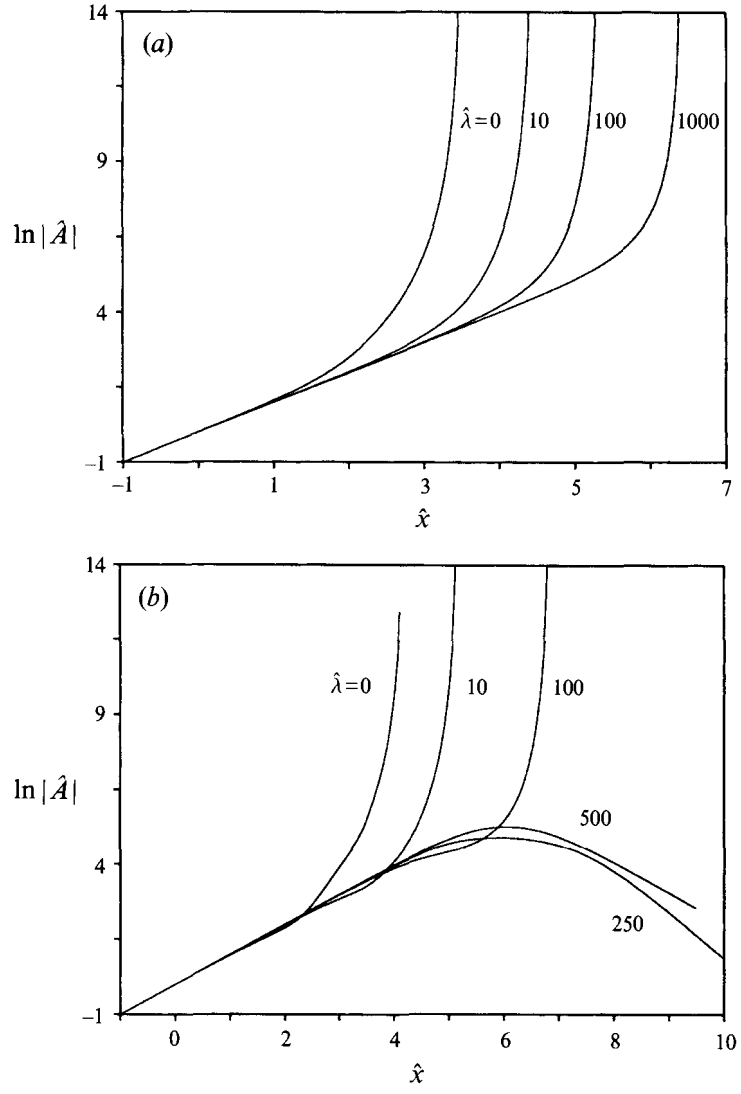

FIGURE 6. Amplitude *vs.* streamwise distance (normalized variables) for an insulated wall with $M = 4$ and various values of the normalized viscous parameter $\hat{\lambda}$: (*a*) $\theta = 60°$; (*b*) $\theta = 30°$.

parameter $\hat{\lambda}$. The results show the expected downstream movement of the singularity and the increase in the linear region with increasing $\hat{\lambda}$. The trends in the physical variables would be the same since the normalization does not depend on the viscous parameter.

In figure 6(*b*) we show the corresponding solutions for $\theta = 30°$. It shows that increasing $\hat{\lambda}$ moves the singularity downstream, eventually eliminating it and causing the amplitude to decay as suggested by the viscous limit analogy. The decaying solutions reach larger amplitudes at larger values of $\hat{\lambda}$ because viscous effects tend to keep the solution linear over a longer streamwise distance.

The special properties of the case when $\theta = 45°$ were discussed in the last section. To provide a basis for later discussion solutions to (4.10) at this wave angle are

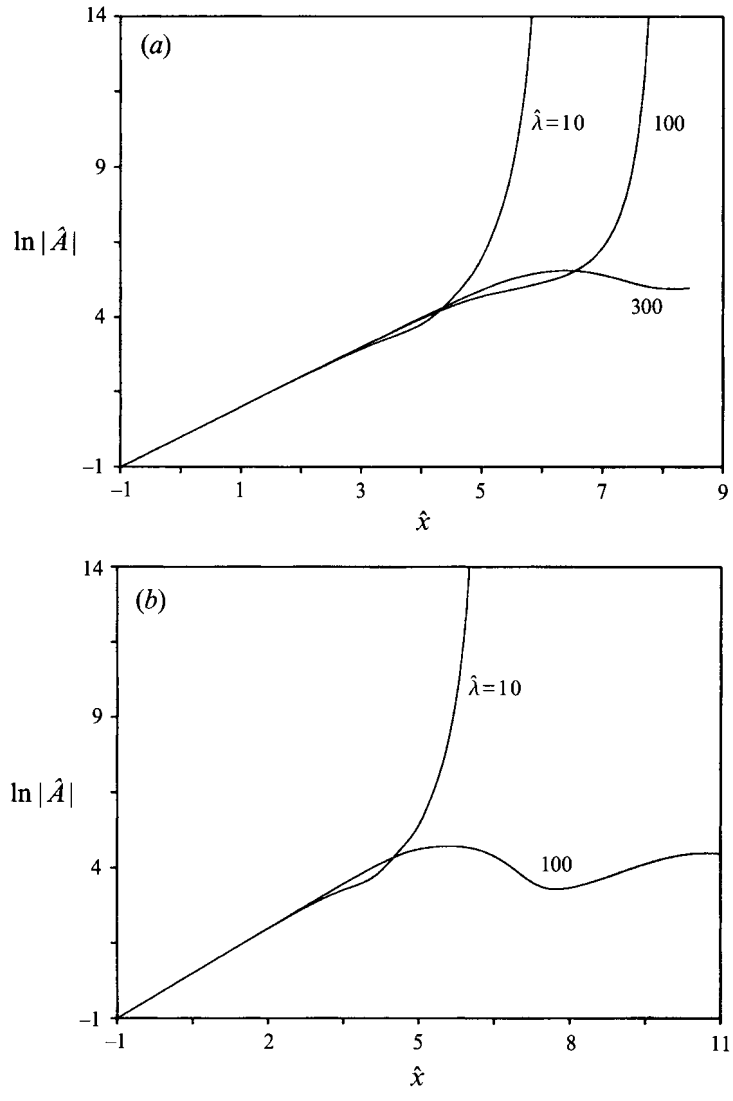

FIGURE 7. Amplitude *vs.* streamwise distance for an insulated wall with $\theta = 45°$ and various values of $\hat{\lambda}$: (*a*) $M = 4$, (*b*) $M = 6$.

shown in figure 7(*a*) for an insulated wall with $M = 4$. The results show that for lower values of $\hat{\lambda}$ the solution is singular but when $\hat{\lambda}$ becomes sufficiently large the amplitude appears to settle into a periodic oscillation. Figure 7(*b*) shows that this can occur at smaller values of $\hat{\lambda}$ for higher Mach numbers. The development of periodic oscillations in the amplitude at $\theta = 45°$ was first observed by WLC. The results of figure 7 however do not exhibit the 'chaotic' transient reported by them due to the values of the coefficients in the supersonic boundary layer case. The periodic behaviour of the amplitude in these cases may continue indefinitely downstream although the reliability of the numerical results comes into question over very long integration distances.

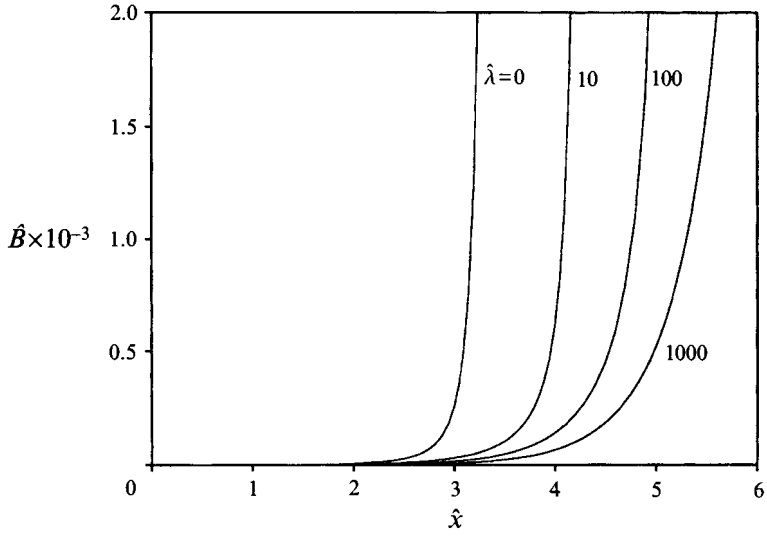

FIGURE 8. Normalized amplitude of the spanwise-dependent mean distortion *vs.* streamwise distance for an insulated wall with $M = 4$, $\theta = 60°$ and various values of $\hat{\lambda}$.

5.3. *Calculation of spanwise-dependent mean distortion component*

A prominent feature of the nonlinear critical layer interaction of a pair of oblique waves is the generation of a spanwise-dependent mean distortion of the velocity and temperature profiles in the outer region at the same order as the fundamental instability. The transverse mode shapes of this component are given by (2.55)–(2.57) subject to (3.35) while the downstream development of its amplitude is given in terms of the fundamental amplitude in (3.36).

Figure 8 shows the evolution of the mean distortion amplitude at a number of values of $\hat{\lambda}$ for an insulated wall with $M = 4$ and $\theta = 60°$. For this case the mean distortion amplitude becomes singular and it can be shown that it has the same asymptotic form near the singularity as the fundamental amplitude. In figure 9 the streamwise velocity and temperature distortion profiles in the outer region multiplied by the amplitude function at various streamwise positions are shown for $\hat{\lambda} = 100$. Both the streamwise velocity and temperature distortions have their peak values at the critical level. For $y > y_c^+$ they decrease and eventually vanish far from the wall. Below the critical level the streamwise velocity decreases from its value at $y = y_c^-$ and approaches a non-zero value at the wall giving a distortion slip velocity which increases as $\hat{x}$ increases. The temperature distortion, on the other hand, goes to zero at the surface of the plate for insulated wall mean conditions. Figure 9 clearly shows the increasing 'jump' in these quantities across the critical layer with increasing $\hat{x}$ in this case.

Figure 10 shows the corresponding distortion amplitude for $\theta = 30°$. At this wave angle the results of figure 6(*b*) showed that the fundamental amplitude decays exponentially due to nonlinear critical layer effects for $\hat{\lambda} = 250$ and 500. The results of figure 10 show that the mean distortion amplitude continues to grow in these cases. This behaviour was first observed by WLC who showed that the distortion amplitude grows linearly (i.e. as $\hat{x}$) while the fundamental amplitude decays exponentially.

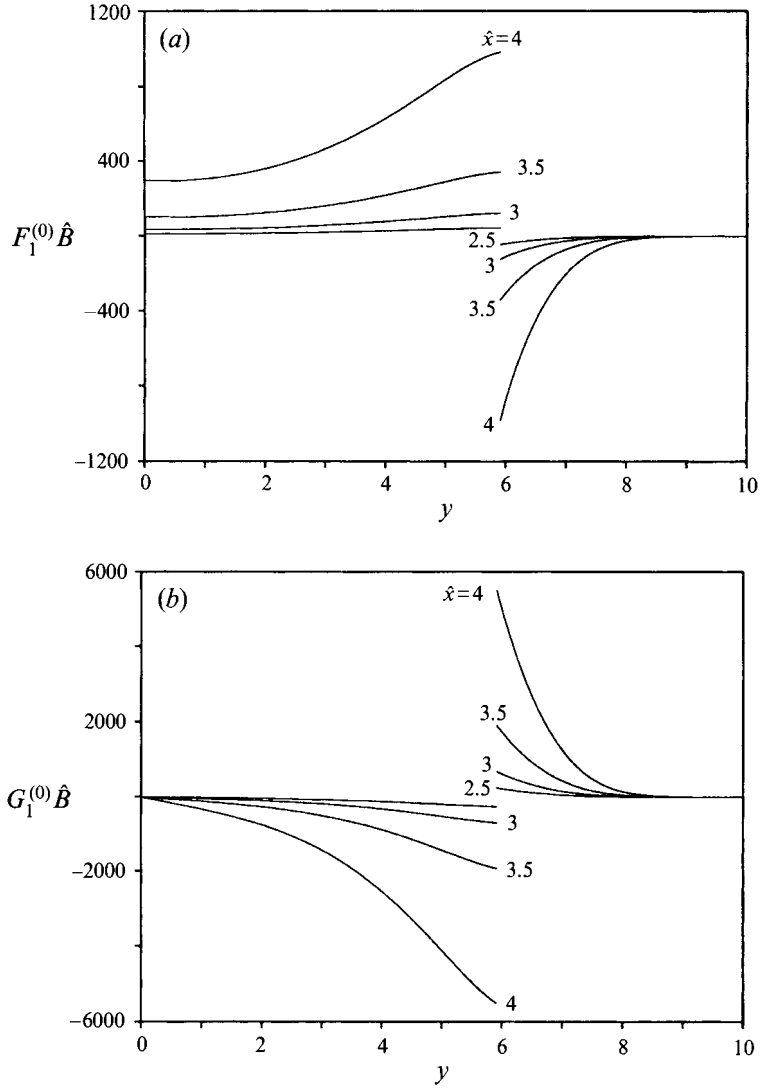

FIGURE 9. Profiles of the spanwise-dependent mean distortion of the (*a*) streamwise velocity and (*b*) temperature at various streamwise positions for an insulated wall with $M = 4$, $\theta = 60°$ and $\hat{\lambda} = 100$.

Figure 11 shows the streamwise velocity and temperature distortion profiles for $\hat{\lambda} = 250$. The profiles are similar to those at $\theta = 60°$ for $y > y_c^+$. For $y < y_c^-$ they have their peak values slightly below the critical level unlike the results of figure 9. The distortion amplitude for $\theta = 45°$ is shown in figure 12. Recalling the results of figure 7(*a*) we see that while the fundamental amplitude appears to have saturated, the distortion amplitude continues to grow.

The development of a large mean distortion or 'streamwise vortex' component is a very important feature of the oblique wave critical layer interaction. It provides a potential mechanism for disrupting the original steady laminar flow even for cases when the oblique wave amplitude does not exhibit explosive growth.

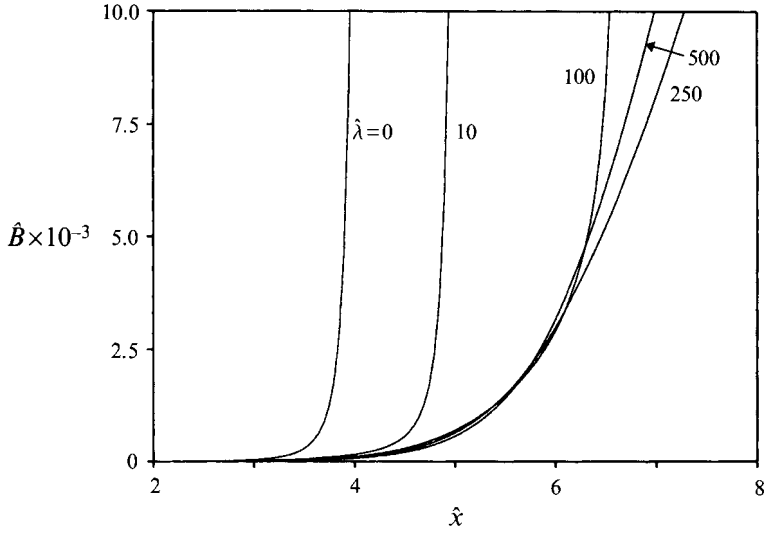

FIGURE 10. Normalized amplitude of the spanwise-dependent mean distortion *vs.* streamwise distance for an insulated wall with $M = 4$, $\theta = 30°$ and various values of $\hat{\lambda}$.

6. Discussion

In this paper we have considered the nonlinear, non-equilibrium critical layer interaction of a pair of oblique instability waves, first considered by GC and extended by WLC, in the context of the supersonic boundary layer flow over a flat plate. The linear stability characteristics of this flow at the moderately high Mach numbers of interest here, namely the preference for oblique, inviscid instability waves, make this the most likely setting in which such an interaction would be observed experimentally.

The critical layer nonlinearity is generic and not dependent upon the particular mean flow being considered which means that the kernel function appearing in the integral nonlinear term is the same as that obtained by GC in the inviscid limit and WLC with viscous effects included in the critical layer. The external linear solution, as well as the linear terms in the critical layer equations, must, of course, be worked out for each case. These linear terms affect the coefficients in the amplitude evolution equation which control the ultimate behaviour of the solution.

We have evaluated the coefficients for the supersonic boundary layer case and computed the corresponding solutions to the amplitude equation. The results show that the growth of the most rapidly growing oblique waves is enhanced by the nonlinear critical layer effects and that the amplitude ends in a singularity at a finite downstream position. This singularity, it was found, cannot be eliminated by viscous effects for wave angles corresponding to the most rapidly growing modes. At other wave angles the nonlinear effects can, given a sufficient amount of viscosity, cause the waves to exhibit exponential decay. This suggests that attempts to force waves at these angles (say, by giving them a larger initial amplitude) could actually be futile since they would be nonlinearly suppressed if the Reynolds number were not large enough.

The appearance of a singularity in the amplitude of course implies that the asymptotic expansions used here break down and that the problem must be rescaled in order to continue to follow the downstream evolution of the flow. From the asymptotic

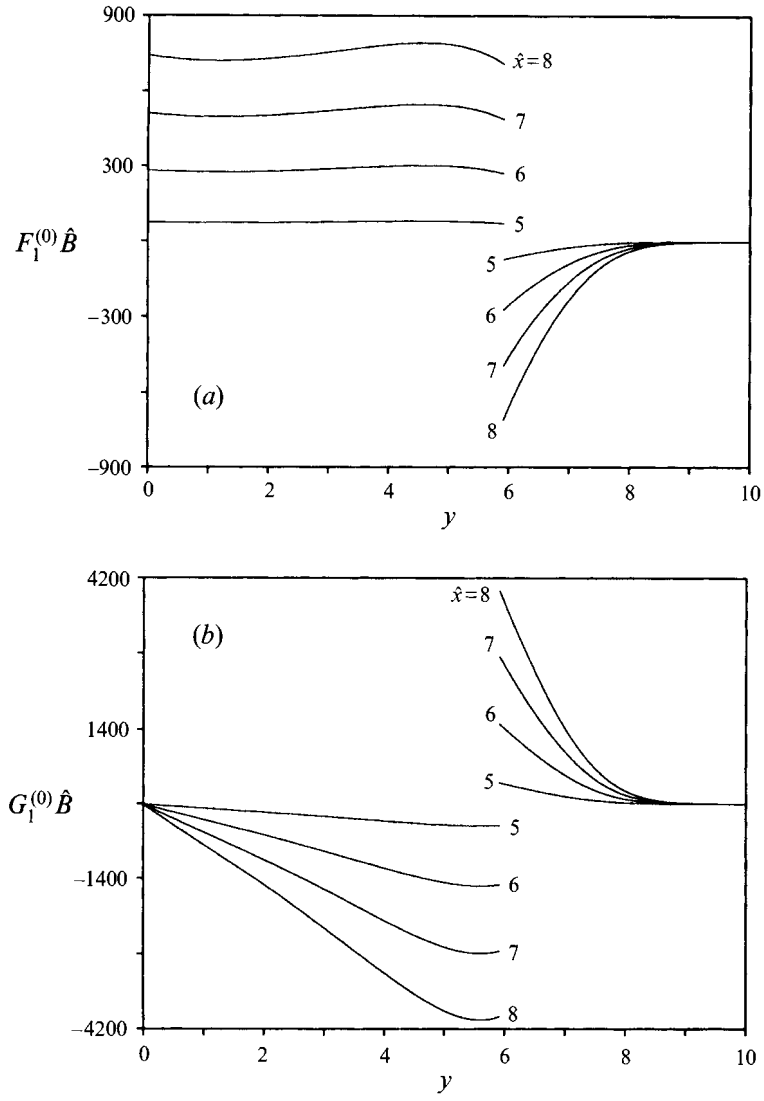

FIGURE 11. Profiles of the spanwise-dependent mean distortion of the (*a*) streamwise velocity and (*b*) temperature at various streamwise positions for an insulated wall with $M = 4$, $\theta = 30°$ and $\hat{\lambda} = 250$.

solution near the singularity GC showed that the next stage of evolution is governed by the full three-dimensional Euler equations in this case. Even for the case where the fundamental disturbance amplitude decays exponetially due to nonlinear critical layer effects the continued growth of the spanwise-dependent mean component amplitude results in a breakdown of the flow structure. In this case the next stage is governed by the linearized Navier–Stokes equations (Goldstein 1994*a*).

The relatively large mean flow distortions produced by the oblique mode critical layer interaction led WLC to seek a connection between the nonlinear critical layer theory and the vortex/wave interaction theory of Hall & Smith (1991) which also features large mean flow changes and near neutral instability waves. A mathematical link between the highly viscous limit of the critical layer amplitude equation and a

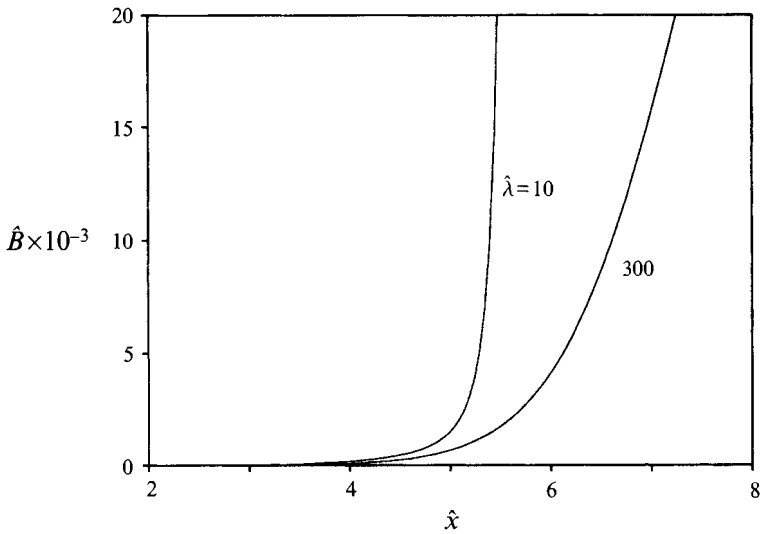

FIGURE 12. Normalized amplitude of the spanwise-dependent mean distortion *vs.* streamwise distance for an insulated wall with $M = 4$, $\theta = 45°$ and various values of $\hat{\lambda}$.

certain limiting form of the weak vortex/wave interaction equation was found. More importantly perhaps, they showed that the nonlinear critical layer solution cannot provide a starting condition to initiate the vortex/wave interaction.

It was shown by Gajjar (1993) that the evolution of a single oblique first mode wave in a supersonic boundary layer is governed by a pair of strongly nonlinear critical layer equations in the low-frequency limit. The resulting amplitude evolution is quite different from that obtained here. In particular the explosive growth associated with the development of a singularity, which we have found to be a dominant feature with a pair of oblique waves, does not occur in the case of a single wave. The ultimate form of the solution for the single wave is difficult to ascertain due to the difficulty of the numerical calculations but the results presented by Gajjar (1993) show that the initial effect of the nonlinearity is to reduce the growth rate from its linear value. Further downstream oscillations set in which may be due to numerical difficulties.

While experimental data are lacking, very recently a number of numerical simulations have been carried out to study possible nonlinear mechanisms in supersonic boundary layer transition. An advantage of the simulations is that the 'background disturbances', in the form of initial conditions, are easily controlled so that a 'quiet' environment can be obtained, something which is particularly difficult to achieve in supersonic wind tunnels.

Bestek *et al.* (1992) introduced a pair of small-amplitude oblique waves at angles of $\pm 45°$ into a supersonic boundary layer with a free stream Mach number of 1.6 and computed the spatial evolution of the flow using the Navier–Stokes equations. Their results showed that, after an initial adjustment region, the oblique waves grow linearly throughout the calculation while a strong spanwise-dependent mean component develops which becomes larger than the oblique waves. The relatively low Mach number and Reynolds number (on the order of 1000 based on the boundary layer thickness) of this simulation makes it relevant for comparison with the highly viscous limit of the nonlinear critical layer theory. In this limit at the wave angle of 45°

the nonlinear term drops out of the equation for the oblique wave amplitude which is then purely linear while, as can be shown from (3.32) and (4.15), the spanwise-dependent mean component is asymptotically larger than the oblique waves (see also Goldstein 1994*a*). These theoretical predictions of the linear growth of the oblique waves and relatively large spanwise dependent mean component are in agreement with the numerical results of Bestek *et al.* (1992).

Numerical simulations for spatially evolving flow at higher Mach numbers are scarce due to the extensive computational resources required. Some preliminary calculations for the spatial evolution of a single wave in a $M = 4.5$ boundary layer were made by Masetrello, Bayliss & Krishnan (1989). Most of the simulations that have been carried to the point of significant nonlinear interactions have considered the temporal evolution of spatially periodic flows. Erlebacher & Hussaini (1990) considered the temporal evolution of a triad consisting of two oblique waves and a two-dimensional wave to study a possible secondary instability route to transition at Mach 4.5 and a Reynolds number based on the boundary layer thickness of 10000. Our interest is in the case where they set the initial two-dimensional amplitude to zero. In this case Erlebacher & Hussaini (1990) obtained faster than linear growth for the oblique waves at $\theta \approx 60°$ as well as the rapid growth of a (0,2) or streamwise vortex component whose amplitude eventually exceeds that of the oblique waves. These results are in agreement with the predictions of the critical layer theory for this wave angle and Mach number.

Other temporal simulations at $M = 4.5$ have used the two-dimensional second mode wave as an initial condition either alone (Erlebacher & Hussaini 1990) or in combination with oblique subharmonic secondary instability modes (Dinavahi, Pruett & Zang 1994). This choice for initial conditions is motivated by the result from linear stability theory that the second mode is the most rapidly growing at this Mach number. As already discussed experimental evidence indicates that (at least for a flat plate boundary layer) the first mode actually dominates the transition process for higher Mach numbers than linear theory would suggest although this will certainly depend on the background disturbance environment. In any case the explosive growth associated with the nonlinear critical layer interaction of a pair of oblique waves, first predicted by the analysis of GC, clearly provides a viable route to transition in moderately supersonic boundary layers. It is hoped that experimental data for this mechanism can be obtained in the not too distant future. In the meantime further numerical simulations of the type referred to above with pairs of oblique waves as initial conditions could provide additional information as to the relative importance of this mechanism in supersonic boundary layer transition.

The authors would like to thank Drs Lennart S. Hultgren and David W. Wundrow for helpful discussions on the linear stability of supersonic boundary layers and Dr Hultgren for the use of his linear stability code. This work was supported by the National Aeronautics and Space Administration, Lewis Research Center under contract number NAS3-27186.

Appendix A. The inner limit of the outer solution

In this appendix we present the inner limit of the outer linear solution which is obtained by substituting $\eta = y - y_c = \epsilon^{1/3} Y$ in the expressions for the linear solutions

in the vicinity of the critical point and taking the limit as ϵ approaches zero:

$$u = \epsilon^{1/3} U_c' Y + \epsilon^{2/3} \left[\tfrac{1}{2} U_c'' Y^2 + a_{1c} x_1 + \sec\theta \cos\beta z \ \mathrm{Re} \left\{ \frac{\sin^2\theta}{Y} A^\dagger + \frac{\mathrm{i}\sin^2\theta}{\alpha U_c'} \frac{1}{Y^2} \left(U_c \frac{\mathrm{d}A^\dagger}{\mathrm{d}x_1} - \mathrm{i}S_1 A^\dagger \right) \right\} \mathrm{e}^{\mathrm{i}\alpha\zeta} \right]$$
$$+ \epsilon \left[\tfrac{1}{6} U_c''' Y^3 + a_{1c}' Y x_1 + \sec\theta \cos\beta z \ \mathrm{Re} \left\{ \left[\sin^2\theta \left(\frac{T_c'}{T_c} - \frac{1}{2} \frac{U_c''}{U_c'} \right) - b_1 \right] A^\dagger + \frac{e_0(x_1)}{Y} \right\} \mathrm{e}^{\mathrm{i}\alpha\zeta} + \cos 2\beta z \ \mathrm{Re} \ f_{1\pm}^{(0)} B^\dagger \right]$$
$$+ \epsilon^{4/3} \left[\tfrac{1}{24} U_c^{(\mathrm{iv})} Y^4 + \tfrac{1}{2} a_{1c}'' Y^2 x_1 + \sec\theta \cos\beta z \ \mathrm{Re} \left\{ \left(-\frac{U_c''}{U_c'} b_1 - \frac{1}{2} \left(\frac{U_c''}{U_c'} \right)^2 + \frac{1}{3} \frac{U_c'''}{U_c'} + \tfrac{1}{2}\alpha^2 - \frac{4a_4}{\bar{\alpha}^2} + \sin^2\theta \left[\frac{1}{4} \left(\frac{U_c''}{U_c'} \right)^2 - \frac{1}{6} \frac{U_c'''}{U_c'} - \frac{1}{2} \frac{U_c''}{U_c'} \frac{T_c'}{T_c} + \frac{1}{2} \frac{T_c''}{T_c} \right] \right) Y A^\dagger \right.$$
$$+ e_1(x_1) \ln|Y| + e_2(x_1) + 2\mathrm{i}\alpha \frac{\mathrm{d}A^\dagger}{\mathrm{d}x_1} \left(b_{2,2}^{\pm} - \frac{1}{\bar{\alpha}^2 \cos^2\theta} b_1 \right)$$
$$\left. - \frac{2\mathrm{i}}{\alpha} \left(U_c \frac{\mathrm{d}A^\dagger}{\mathrm{d}x_1} - \mathrm{i}S_1 A^\dagger \right) \left(b_{2,1}^{\pm} - \frac{U_c''}{2U_c'^2} b_1 \right) \right\} \mathrm{e}^{\mathrm{i}\alpha\zeta} + \cos 2\beta z \ \mathrm{Re} \ f_{2\pm}^{(0)} Y B^\dagger \Big] + \cdots, \tag{A 1}$$

$$v = \epsilon \left[-\bar{\alpha} \cos\beta z \ \mathrm{Re} \ \mathrm{i}A^\dagger \mathrm{e}^{\mathrm{i}\alpha\zeta} - a_{2c} \right] + \epsilon^{4/3} \cos\beta z \ \mathrm{Re} \ \mathrm{i}\bar{\alpha} b_1 Y A^\dagger \mathrm{e}^{\mathrm{i}\alpha\zeta} + \cdots, \tag{A 2}$$

$$w = -\sin\theta \sin\beta z \left[\epsilon^{2/3} \ \mathrm{Re} \ \frac{\mathrm{i}A^\dagger \mathrm{e}^{\mathrm{i}\alpha\zeta}}{Y} + \epsilon \ \mathrm{Re} \left(\frac{T_c'}{T_c} - \frac{U_c''}{2U_c'} \right) \mathrm{i}A^\dagger \mathrm{e}^{\mathrm{i}\alpha\zeta} \right.$$
$$\left. - \epsilon^{4/3} \ \mathrm{Re} \left(\tfrac{1}{2}\bar{\alpha}^2 + \frac{1}{6} \frac{U_c'''}{U_c'} - \frac{1}{4} \left(\frac{U_c''}{U_c'} \right)^2 + \frac{1}{2} \frac{U_c''}{U_c'} \frac{T_c'}{T_c} - \frac{1}{2} \frac{T_c''}{T_c} \right) Y \mathrm{i}A^\dagger \mathrm{e}^{\mathrm{i}\alpha\zeta} \right] + \cdots, \tag{A 3}$$

$$p = 1 + \gamma M^2 \cos\theta \frac{U_c'}{T_c} \cos\beta z \left[\epsilon \ \mathrm{Re} \ A^\dagger \mathrm{e}^{\mathrm{i}\alpha\zeta} + \epsilon^{4/3} \ \mathrm{Re} \left\{ \frac{2\mathrm{i}c_{2,1}}{\bar{\alpha}\cos\theta} \left(U_c \frac{\mathrm{d}A^\dagger}{\mathrm{d}x_1} - \mathrm{i}S_1 A^\dagger \right) - 2\mathrm{i}\alpha c_{2,2} \frac{\mathrm{d}A^\dagger}{\mathrm{d}x_1} \right\} \mathrm{e}^{\mathrm{i}\alpha\zeta} \right] + \cdots, \tag{A 4}$$

$$T = T_c + \epsilon^{1/3} T_c' Y + \epsilon^{2/3} \left[\tfrac{1}{2} T_c'' Y^2 + a_{3c} x_1 + \frac{1}{Y} \frac{T_c'}{U_c'} \sec\theta \cos\beta z \ \mathrm{Re} \ A^\dagger \mathrm{e}^{\mathrm{i}\alpha\zeta} \right]$$
$$+ \epsilon \left[\tfrac{1}{6} T_c''' Y^3 + a_{3c}' Y x_1 \right.$$
$$+ \cos\beta z \ \mathrm{Re} \left\{ \frac{T_c'}{U_c' \cos\theta} \left(-b_1 + \frac{T_c''}{T_c'} - \frac{1}{2} \frac{U_c''}{U_c'} \right) + (\gamma - 1) M^2 U_c' \cos\theta \right\} A^\dagger \mathrm{e}^{\mathrm{i}\alpha\zeta}$$
$$\left. + \cos 2\beta z \ \mathrm{Re} \ g_{1\pm}^{(0)} B^\dagger \right] + \cdots, \tag{A 5}$$

where $f_{1\pm}^{(0)}, f_{2\pm}^{(0)}$ and $g_{1\pm}^{(0)}$ are constants that take on different values above and below the critical level.

Appendix B. Definition of terms appearing in the critical layer equations

The constants appearing in the leading-order critical layer equations (3.17) and (3.19) are defined as

$$\phi_1 = U_c' \left(\lambda \mu_c' T_c' T_c - a_{2c}\right), \tag{B 1}$$

and

$$\tau_1 = -T_c' a_{2c} + \lambda \left(U_c'^2 (\gamma - 1) M^2 \mu_c + \mu_c' T_c T_c'^2\right). \tag{B 2}$$

The inhomogeneous viscous terms in equations (3.21)–(3.23) are

$$\begin{aligned}\mathscr{U}_2 = {} & \lambda U_c' \mu_c \left(1 - \frac{\mu_c' T_c}{\mu_c}\right) \tilde{T}_{1YY} - \lambda T_c' \mu_c \left(1 + \frac{\mu_c' T_c}{\mu_c}\right) Y \tilde{u}_{1YYY} \\ & - \lambda T_c' \mu_c \left(1 + 2\frac{\mu_c' T_c}{\mu_c}\right) \tilde{u}_{1YY} + \lambda (\gamma - 1) M^2 \mu_c U_c'^3 \lambda U_c' T_c \mu_c'' T_c'^2,\end{aligned} \tag{B 3}$$

$$\mathscr{W}_2 = \lambda T_c \mu_c' T_c' \tilde{w}_{1Y} + \lambda \mu_c T_c' \left(1 + \frac{\mu_c' T_c}{\mu_c}\right) Y \tilde{w}_{1YY}, \tag{B 4}$$

and

$$\begin{aligned}\mathscr{T}_2 = {} & \lambda (\gamma - 1) M^2 \left(2 \mu_c U_c' \tilde{u}_{1Y} + \mu_c' T_c' U_c'^2 Y\right) \\ & + \lambda \left[\mu_c' T_c'^3 \left(1 + \frac{\mu_c'' T_c}{\mu_c'}\right) Y + \mu_c T_c' \left(1 + \frac{\mu_c' T_c}{\mu_c}\right) Y \tilde{T}_{1YY} + 2 T_c \mu_c' T_c' \tilde{T}_{1Y}\right].\end{aligned} \tag{B 5}$$

The constant appearing in the critical layer vorticity equation (3.25) is given as

$$\phi_3 = \sec\theta \left\{\frac{U_c'''}{U_c'} - \frac{T_c''}{T_c} - \left(\frac{U_c''}{U_c'}\right)^2 - \frac{U_c''}{U_c'} b_1 + \left(\frac{T_c'}{T_c}\right)^2 + \tfrac{1}{2}(\bar{\alpha}^2 - \alpha^2) + \tfrac{1}{2}\bar{\alpha}^2 \sin^2\theta\right\}. \tag{B 6}$$

Appendix C. Exponential factors in the kernel function

In this appendix we define the exponential functions appearing in the viscous kernel function (4.2)–(4.5).

$$\chi_1(\xi_1, \xi_2, \xi_3, \bar{x}) = \exp\left(-\bar{\lambda} (\xi_2 - \xi_3)^2 \left[(\bar{x} - \xi_1) - \tfrac{2}{3}(\xi_2 - \xi_3)\right]\right), \tag{C 1}$$

$$\begin{aligned}\chi_2(\xi_1, \xi_2, \xi_3, \bar{x}) = {} & \exp\left(-\bar{\lambda} \left\{(\xi_1 - \xi_3)\left[\tfrac{1}{3}(\xi_1 - \xi_3)^2 + (\bar{x} - \xi_1)^2\right.\right.\right. \\ & \left.\left.\left. + (\bar{x} - \xi_1)(\xi_1 - \xi_3) - (\bar{x} - \xi_2)^2\right]\right\}\right) \\ & \times \exp\left(-\bar{\lambda} \left\{(\xi_1 - \xi_2)^2 \left[\tfrac{1}{3}(\xi_1 - \xi_2) + (\bar{x} - \xi_1)\right] + \tfrac{1}{3}(\xi_3 - \xi_2)^3\right\}\right),\end{aligned} \tag{C 2}$$

$$\chi_3(\xi_1, \xi_2, \xi_3, \bar{x}) = \exp\left(-\bar{\lambda} (\bar{x} - \xi_1)(\xi_1 - \xi_3)^2\right), \tag{C 3}$$

$$\begin{aligned}\chi_4(\xi_1, \xi_2, \xi_3, \bar{x}) = {} & \exp\left(-\bar{\lambda} \left\{(\xi_1 - \xi_2)^2 \left[\bar{x} - \xi_1 + \tfrac{2}{3}(\xi_1 - \xi_2)\right] + \tfrac{4}{3}(\xi_3 - \xi_1)^3\right\}\right) \\ & \times \exp\left(-\bar{\lambda} \left\{(\xi_3 - \xi_1)^2 [2\bar{x} + \xi_1 - 3\xi_2]\right.\right. \\ & \left.\left. + 2\,(\xi_1 - \xi_2)(\xi_3 - \xi_1)(\bar{x} - \xi_2)\right\}\right),\end{aligned} \tag{C 4}$$

$$\begin{aligned}\chi_5(\xi_1, \xi_2, \xi_3, \xi_4, \bar{x}) = {} & \exp\left(-\bar{\lambda} \left\{(\bar{x} - \xi_1)(\xi_3 - \xi_1)^2\right.\right. \\ & \left.\left. + (\xi_3 - \xi_4)^2 \left[\bar{x} - \xi_1 + \tfrac{2}{3}(\xi_3 - \xi_4)\right]\right\}\right),\end{aligned} \tag{C 5}$$

$$\chi_6(\xi_1,\xi_2,\xi_3,\xi_4,\bar{x}) = \exp\left(-\bar{\lambda}(\xi_1-\xi_2)^2\left[\tfrac{2}{3}(\xi_1-\xi_2)+\bar{x}-\xi_1+2(\xi_3-\xi_1)\right]\right)$$
$$\times\exp\left(-\bar{\lambda}(\xi_3-\xi_1)^2\left[\tfrac{4}{3}(\xi_3-\xi_1)+2(\bar{x}-\xi_1)+3(\xi_1-\xi_2)\right]\right)$$
$$\times\exp\left(\bar{\lambda}\left\{(\xi_3-\xi_4)^2\left[\tfrac{2}{3}(\xi_3-\xi_4)+(\xi_1-\xi_2)\right]\right.\right.$$
$$\left.\left.-2(\bar{x}-\xi_1)(\xi_1-\xi_2)(\xi_3-\xi_1)\right\}\right), \tag{C 6}$$

$$\chi_7(\xi_1,\xi_2,\xi_3,\xi_4,\bar{x}) = \exp\left(-\bar{\lambda}\left\{(\xi_1-\xi_2)^2\left[\tfrac{2}{3}(\xi_1-\xi_2)\right.\right.\right.$$
$$\left.\left.+(\bar{x}-\xi_1)\right]+(\bar{x}-\xi_2)(\xi_3-2\xi_2+\xi_1)(\xi_3-\xi_1)\right\}\right)$$
$$\times\exp\left(-\bar{\lambda}(\xi_3-\xi_4)^2\left[\tfrac{2}{3}(\xi_3-\xi_4)+(\bar{x}-\xi_2)\right]\right). \tag{C 7}$$

REFERENCES

BALAKUMAR, P. & MALIK, M. R. 1992 Waves produced from a harmonic point source in a supersonic boundary layer flow. *J. Fluid Mech.* **245**, 229–247.

BESTEK, H., THUMM, A. & FASEL, H. 1992 Numerical investigation of later stages of transition in transonic boundary layers. *First European Forum on Laminar Flow Technology, March* 16–18, 1992.

CHANG, C.-L. & MALIK, M. R. 1992 Oblique mode breakdown in a supersonic boundary layer using nonlinear PSE. In *Instability, Transition and Turbulence* (ed. M.Y. Hussaini, A. Kumar & C.L. Street). Springer.

DEMETRIADES, A. 1960 An experiment on the stability of hypersonic laminar boundary layers. *J. Fluid Mech.* **7**, 385–396.

DINAVAHI, S. P. G., PRUETT, C. D. & ZANG, T. A. 1994 Direct numerical simulation and data analysis of a Mach 4.5 transitional boundary layer flow. *Phys. Fluids* **6**, 1323–1330.

DUNN, D. W. & LIN, C. C. 1955 On the stability of the laminar boundary layer in a compressible fluid *J. Aero. Sci.* **22**, 455–477.

ERLEBACHER, G. & HUSSAINI, M. Y. 1990 Numerical experiments in supersonic boundary layer stability. *Phys. Fluids* A **2**, 94–104.

GAJJAR, J. S. B. 1993 Nonlinear evolution of the first mode supersonic oblique waves in compressible boundary layers. Part I - Heated /Cooled walls. *NASA Tech. Mem.* 106087.

GOLDSTEIN, M. E. 1994*a* Nonlinear interactions between oblique instability waves on nearly parallel shear flows. *Phys. Fluids* **6**, 724–735.

GOLDSTEIN, M. E. 1994*b* The role of critical layers in the nonlinear stage of boundary layer transition. Submitted to *Proc. R. Soc. Lond.* A.

GOLDSTEIN, M. E. & CHOI, S.-W. 1989 Nonlinear evolution of interacting oblique waves on two dimensional shear layers. *J. Fluid Mech.* **207**, 97–120 and Corrigendum, *J. Fluid Mech.* **216**, 1990, 659 (referred to herein as GC).

GOLDSTEIN, M. E. & LEE, S. S. 1992 Fully coupled resonant–triad interaction in an adverse-pressure-gradient boundary layer. *J. Fluid Mech.* **245**, 523–551.

GOLDSTEIN, M. E. & LEIB, S. J. 1989 Nonlinear evolution of oblique waves on compressible shear layers. *J. Fluid Mech.* **207**, 73–96.

HALL, P. & SMITH, F. T. 1991 On strongly nonlinear vortex/wave interactions in boundary layer transition. *J. Fluid Mech.* **227**, 641–666.

HICKERNELL, F. J. 1984 Time dependent critical layers in shear flows on the beta-plane. *J. Fluid Mech.* **142**, 431–449.

KENDALL, J. M. 1975 Wind tunnel experiments relating to supersonic and hypersonic boundary layer transition. *AIAA J.* **13**, 290–299.

KOSINOV, A. D., MASLOV, A. A. & SHEVELKOV, S. G. 1990 Experiments on the stability of supersonic laminar boundary layers. *J. Fluid Mech.* **219**, 621–633.

LAUFER, J. & VREBALOVICH, T. 1960 Stability and transition of a supersonic laminar boundary layer on an insulated flat plate. *J. Fluid Mech.* **9**, 257–299.

LEES, L. 1947 The stability of the laminar boundary layer in a compressible fluid. *NACA Rep.* 876.

LEES, L. & LIN, C.C. 1946 Investigation of the stability of the laminar boundary layer in a compressible fluid. *NACA TN* 1115.

LEES, L. & RESHOTKO, E. 1962 Stability of the compressible laminar boundary layer. *J. Fluid Mech.* **12**, 555–590.

LEIB, S.J. 1991 Nonlinear evolution of subsonic and supersonic disturbances on a compressible free shear layer. *J. Fluid Mech.* **224**, 551–578.

LYSENKO, V.I. & MASLOV, A.A. 1984 The effect of cooling on supersonic boundary layer stability. *J. Fluid Mech.* **147**, 39–52.

MACK, L.M. 1975 Linear stability theory and the problem of supersonic boundary-layer transition. *AIAA J.* **13**, 278–289.

MACK, L.M. 1984 Boundary layer stability theory. In *Special Course on Stability and Transition of Laminar Flow. AGARD Rep.* 709.

MACK, L.M. 1987 Review of linear compressible stability theory. In *Stability of Time Dependent and Spatially Varying Flows* (ed. D.L. Dwoyer & M.Y. Hussaini). Springer.

MAESTRELLO, L., BAYLISS, A. & KRISHNAN, R. 1989 Numerical study of three dimensional spatial instability of a supersonic flat plate boundary layer. *ICASE Rep.* 89–74.

MALIK, M.R. 1989 Prediction and control of transition in supersonic and hypersonic boundary layers. *AIAA J.* **27**, 1487–1493.

NG, L.L. & ZANG, T.A. 1993 Secondary instability mechanisms in compressible axisymmetric boundary layers. *AIAA J.* **31**, 1605–1610.

RESHOTKO, E. 1960 Stability of the compressible laminar boundary layer. *GALCIT Memo* 52. Calif. Inst. of Technology, Pasadena, CA.

RESHOTKO, E. 1969 Stability theory as a guide to the evaluation of transition data. *AIAA J.* **7**, 1086–1091.

WU, X., LEE, S.S. & COWLEY, S.J. 1993 On the weakly nonlinear three-dimensional instability of shear layers to pairs of oblique waves; the Stokes layer as a paradigm. *J. Fluid Mech.* **253**, 681–721 (referred to herein as WLC).